



POLITECNICO
MILANO 1863

SCUOLA DI INGEGNERIA INDUSTRIALE
E DELL'INFORMAZIONE

Dynamic analysis of land-based SMR RITM-200 and passive residual heat removal system

TESI DI LAUREA MAGISTRALE IN
NUCLEAR ENGINEERING
INGEGNERIA NUCLEARE

Author: **Artem Gaganov**

Student ID: 988164

Advisor: Prof. Marco Enrico Ricotti

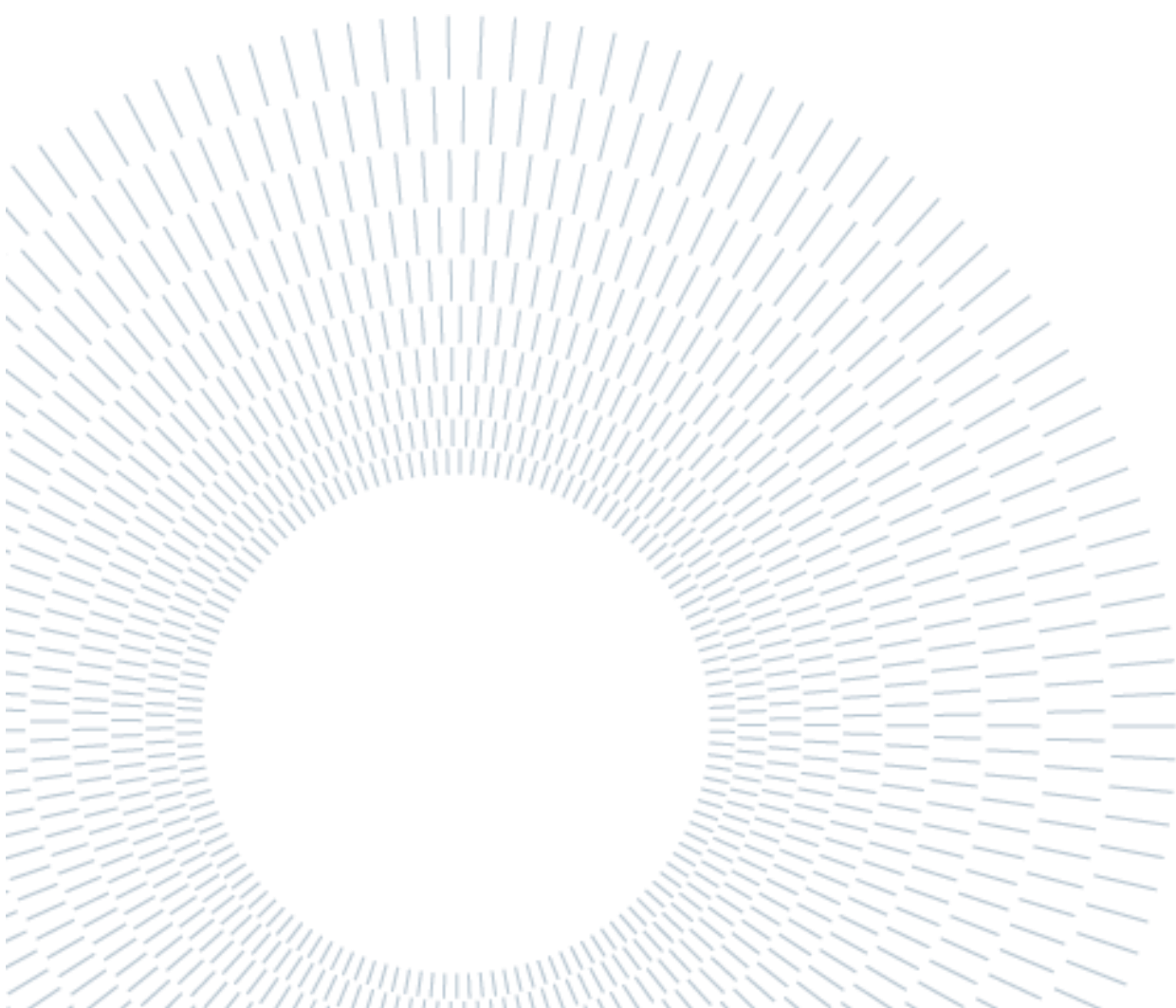
Co-advisor: Prof. Stefano Lorenzi

Academic Year: 2023-24

Abstract

This thesis presents a comprehensive dynamic analysis of the RITM-200 small modular reactor (SMR) and its passive residual heat removal system. Using Modelica language with the Dymola simulation environment, simulations were conducted to assess the behavior of both the primary circuit and balance of plant of the RITM-200 reactor under dynamic conditions. For the dynamic analysis of the primary and secondary sides of the RITM-200 reactor, the chosen transient scenario was the "load following" mode, wherein the nominal power was decreased by 10%. This allowed for a detailed examination of the reactor's response and performance under varying power demands. Furthermore, the thesis investigates the dynamic performance and sizing of the passive residual heat removal system under the assumption that all control rods are inserted. The passive system is tasked with removing residual power using air and water heat exchangers. Through rigorous simulation and analysis, insights into the effectiveness and reliability of this passive system in mitigating residual heat in emergency scenarios were obtained. The findings from this research contribute to a better understanding of the dynamic behavior of the RITM-200 SMR and its passive safety systems. This knowledge is vital for ensuring the safe and efficient operation of small modular reactors in practical applications.

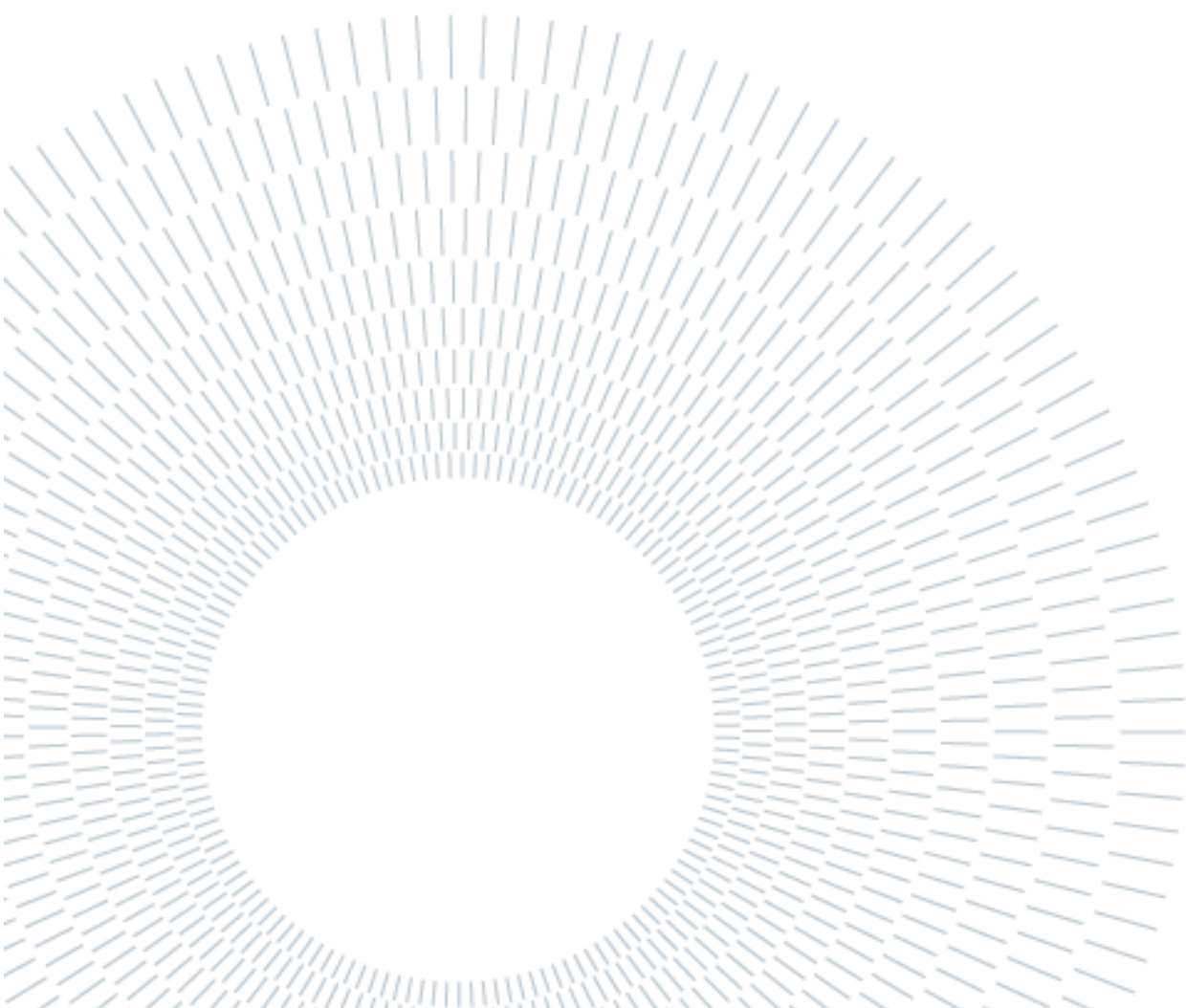
Keywords: SMR RITM-200, Dynamic Analysis, Passive Residual Heat Removal System, Modelica, Load Following, Safety Analysis.



Abstract in lingua italiana

Questa tesi presenta un'analisi dinamica completa del RITM - 200 small modular reactor (SMR) e del suo sistema passivo di rimozione del calore residuo. Utilizzando il linguaggio Modelica con l'ambiente di simulazione Dymola, sono state condotte simulazioni per valutare il comportamento sia del circuito primario che dell'equilibrio dell'impianto del reattore RITM-200 in condizioni dinamiche. Per l'analisi dinamica dei lati primario e secondario del reattore RITM-200, lo scenario transitorio scelto era la modalità "load following", in cui la potenza nominale era diminuita del 10%. Ciò ha permesso un esame dettagliato della risposta e delle prestazioni del reattore in base alle diverse esigenze di potenza. Inoltre, la tesi indaga le prestazioni dinamiche e il dimensionamento del sistema passivo di rimozione del calore residuo nell'ipotesi che tutte le barre di controllo siano inserite. Il sistema passivo ha il compito di rimuovere la potenza residua utilizzando scambiatori di calore aria e acqua. Attraverso rigorose simulazioni e analisi, sono state ottenute informazioni sull'efficacia e l'affidabilità di questo sistema passivo nel mitigare il calore residuo in scenari di emergenza. I risultati di questa ricerca contribuiscono a una migliore comprensione del comportamento dinamico del RITM-200 SMR e dei suoi sistemi di sicurezza passiva. Questa conoscenza è vitale per garantire il funzionamento sicuro ed efficiente di piccoli reattori modulari in applicazioni pratiche.

Parole chiave: SMR RITM-200, Analisi dinamica, Sistema passivo di rimozione del calore residuo, Modelica, Load Following, Analisi di sicurezza.



Contents

| | |
|---|-----|
| Abstract..... | i |
| Abstract in lingua italiana..... | iii |
| Contents..... | v |
| 1 Introduction..... | 1 |
| 2 Economics of SMR..... | 3 |
| 3 Rosatom’s projects..... | 5 |
| 3.1 Offshore projects..... | 5 |
| 3.1.1 OK-150..... | 6 |
| 3.1.2 OK-900..... | 7 |
| 3.1.3 KLT-40..... | 7 |
| 3.1.4 RITM-200..... | 8 |
| 3.1.5 RITM-400..... | 9 |
| 3.2 Onshore projects..... | 10 |
| 4 Safety requirements for RITM-200..... | 12 |
| 4.1 Emergency cooling system (PRHRS)..... | 13 |
| 5 Description of components of RITM-200..... | 14 |
| 5.1 Steam generator unit (SGU)..... | 16 |
| 5.2 Reactor core..... | 17 |
| 5.3 Steam generator..... | 19 |
| 5.4 Pump..... | 22 |
| 5.5 CPS drives..... | 23 |
| 5.6 Pressurizer..... | 23 |
| 5.7 Turbine..... | 23 |
| 6 Modeling of RITM-200 system..... | 48 |
| 6.1 Reactor core..... | 49 |
| 6.1.1 Neutronics..... | 50 |
| 6.1.2 Thermal modelling..... | 52 |
| 6.1.3 Hydraulic model of coolant..... | 53 |
| 6.1.4 Other components of primary circuits..... | 55 |

| | |
|--|----|
| 6.2 Steam generator | 55 |
| 6.3 Secondary side model | 57 |
| 6.4 Passive residual heat removal model..... | 62 |
| 7 Results of modelling..... | 69 |
| 7.1 Steady state simulation of primary and secondary circuits..... | 69 |
| 7.2 Load following simulation | 70 |
| 7.3 Passive residual heat removal simulation | 73 |
| 8 Conclusion and future developments..... | 54 |
| Bibliography | 55 |
| List of Figures..... | 57 |
| List of Tables..... | 59 |
| List of symbols | 60 |
| Acknowledgments..... | 65 |

1 Introduction

Economic development and population growth consistently drive the demand for a reliable and ever-increasing supply of energy. Nuclear power stands out as one of the most dependable and sustainable technologies for power generation. This energy source offers the advantage of generating affordable electricity that is not influenced by weather conditions or economic fluctuations. Traditionally, most commercial Nuclear Power Plants (NPPs) produce high electrical power outputs. However, recent trends in power generation are shifting towards smaller units. These smaller units are better suited for supplying electricity to remote locations, creating more distributed energy systems, and purifying drinking water. [1]

Small modular reactors (SMRs) are generally defined as nuclear reactors with power outputs between 10 megawatts electric (MWe) and 300 MWe. SMRs present several technical features that enhance construction predictability and lead to potential reductions in construction costs and delivery times in comparison with large nuclear power plants (LNPP). [2]

According to the International Atomic Energy Agency (IAEA), approximately 70 SMR concepts are currently under development, which represents a 40% increase from 2018. [2] While the term “SMR” has been adopted around the world to refer to all small reactor designs, significant differences remain across the major types of SMRs under development.

The most mature Small Modular Reactor (SMR) concepts proposed by vendors are evolutionary variants of light water Generation II and Generation III/III+ reactors (LWR-SMRs), which are already operating worldwide. These designs benefit from many decades of operational and regulatory experience and represent approximately 50% of the SMR designs currently under development.

The acronym SMR stands for Small Modular Reactor, emphasizing its compact size and modular construction. SMRs are designed to be built and assembled in a factory, then shipped to their final location. Due to their smaller power output, SMRs are particularly suitable for areas with smaller power grids or remote locations, where connecting to the existing power grid would be economically unfeasible. For example, OKBM Afrikantov has designed a reactor that will be placed on a boat, creating a floating nuclear power plant. This innovative approach allows the power station to be easily relocated, providing energy wherever it is needed.

The SMRs are under development in the following countries: Argentina, Brazil, Canada, China, France, India, Japan, Republic of Korea, Russian Federation, South Africa and the USA. Almost every country is developing a Light Water Reactor (LWR) but it is possible to observe that Liquid Metal Cooled Reactors (LMCRs) and Gas Cooled Reactors (GCRs) started to be popular concepts. [1]

Despite differences in designs all SMRs should secure:

- Inherent and passive safety features to assure security during operation and accident conditions.

- Proliferation resistance.
- Economic competitiveness with other power generation technology.
- Probability of severe accident below 10^{-5} .
- Ease of operation and maintenance.
- Transportability from the factory to the field.

Classification of SMRs according to generation, neutron spectrum and coolant is shown in Figure 1.

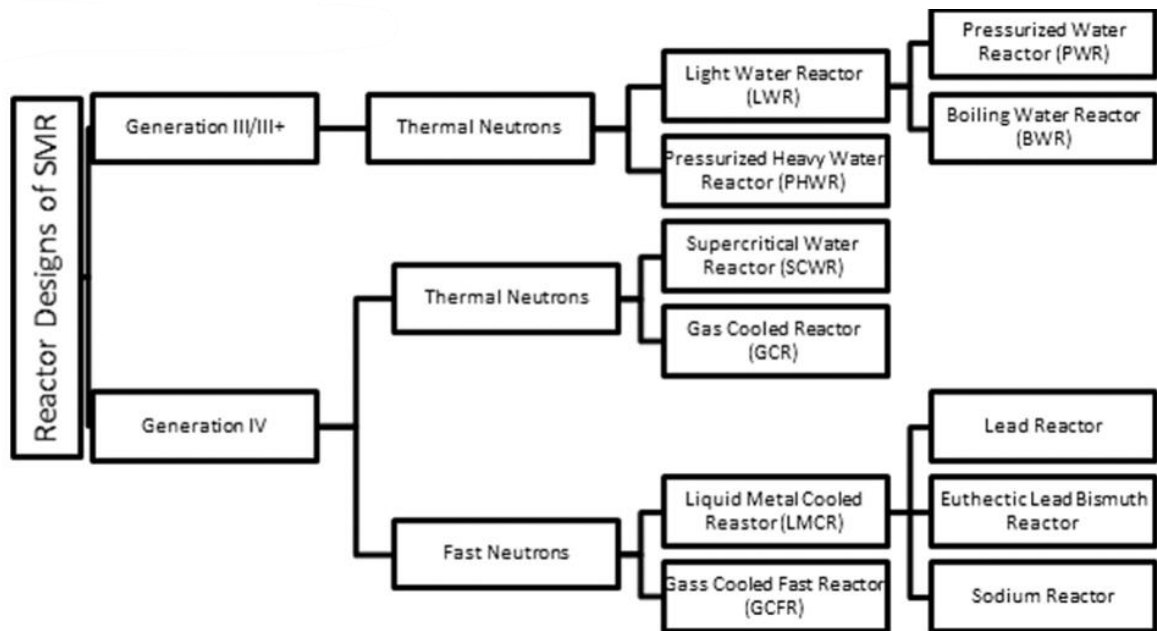


Figure 1: Classification of SMR [1]

A common feature of all SMRs, compared to larger units, is their smaller power density. This means that the amount of heat needing to be removed relative to the surface area is smaller, making it possible to use passive cooling systems to maintain heat removal from the reactor vessel. Another advantage of the integrated design is the elimination of large Loss of Coolant Accidents (LOCA), thanks to the small diameter of the pipes that leave the vessel and reduced number of pipes. [1]

The aim of this thesis is to investigate the conceptual design of a ground-based small nuclear power plant (SNPP) RITM-200 reactor, originally used in universal nuclear icebreakers. The primary objective is to illustrate the "load following" capability of the reactor. The second goal is to perform a dynamic analysis of the Passive Residual Heat Removal System (PRHRS) in the event of full control rod insertion. The modeling is performed using the Dymola simulation environment.

Before explanation of the RITM-200 model, the paper describes economics features of SMR and the history of Rosatom's projects.

2 Economics of SMR

SMRs typically boast attractive characteristics such as simplicity, enhanced safety, and requiring limited financial resources. However, they are often not considered economically competitive with large reactors (LR) due to the accepted axiom "bigger is better," which applies the principle of economy of scale. According to this principle, the specific capital cost (currency/kWe) of a nuclear reactor decreases with increasing size, as the rate reduction of unique setup costs in investment activities (e.g., licensing, siting activities, or civil works to access the transmission network) is achieved. As a result, in large, developed countries, reactor sizes have steadily increased from a few hundred MWe to 1500 MWe and more over the last four decades. However, the economies of scale apply only when comparing one large reactor to one small reactor of a similar design, as has largely been the case in the past. Today, this comparison is no longer valid, as smaller, modular reactors have very different designs and characteristics from their large-scale counterparts. [3]

By contrast, SMRs exhibit several benefits that can only be replicated by LRs to a very limited extent. In order to achieve serial factory fabrication, the market for a single design must be sufficiently large, highlighting the potential benefits of developing such a global market. There are several factors allowing SMR to be economically competitive with LR: modularization, design simplification, standardization, harmonization. Their impact on decrease of levelized cost of electricity (LCOE) is presented on the Fig. 2. [2]

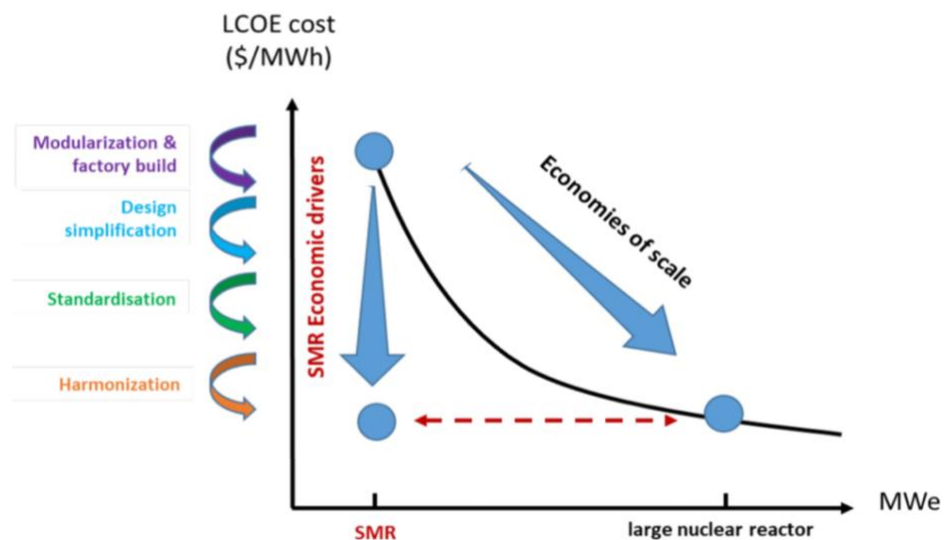


Figure 2: SMR key economic drivers to compensate for diseconomies of scale [2]

Short description of each factor:

- **Design simplification:** The unique physical features of smaller cores in terms of enhanced passive mechanisms and higher design integration offer new opportunities for the simplification of SMR systems. Some active components, for example reactor cooling pumps and their associated auxiliary systems, may no longer be necessary in novel SMR designs, which represents an important advantage compared to current large LWR designs. These different simplification approaches could translate into lower

construction costs for SMRs, both directly through a reduction in the number and size of components and systems, and indirectly through benefits at the project management level. Moreover, it could lead to a reduction in the risks associated with rework, as well as a reduction in the delays during construction.

- **Standardization:** SMR designs provide higher levels of standardization. Standardization of design, and its subsequent replication, has proven to be an effective way to drive costs down for large reactors as it fosters learning by doing and contributes to the mobilization of the supply chain through long-term new build programs.
- **Modularization:** Modularization is a way of simplifying construction by splitting the plant up into packages (modules) that can be factory-built, transported, and then assembled on-site. Although modular construction has been used for large nuclear power plants, SMRs can even further capitalize on the benefits of modular construction approaches. Cost reductions from modularization can be expected from construction and/or pre-assembly of modules away from the construction site in a dedicated factory, where labor productivity and quality control can be expected to be higher and project management risks lower.

The benefits of modular construction have been well-documented in other industries, such as shipbuilding and aircraft construction, where modularization of construction in factories has resulted in cost reductions. General observations of modularization in the power sector indicate lead-time reductions of 30% and 20% in terms of lower costs. For the construction of nuclear reactors, modularization and factory fabrication is already applicable to about 30% of the construction and could increase to up to 60-80% with the adoption of the more ambitious strategies enabled by the reduced size of the components.

The key advantages of SMRs, which can benefit consumers and humanity in general, are illustrated in Fig. 3. SMRs can be considered for a wide range of potential sites, including those in extreme climate zones or areas lacking access to grid infrastructure [4]. In addition to onshore solutions, floating SMR power plants offer ultimate flexibility in supplying power to remote offshore or coastal sites. Moreover, SMR units can synergize with renewable energy systems due to their ability to operate in a load-following mode.

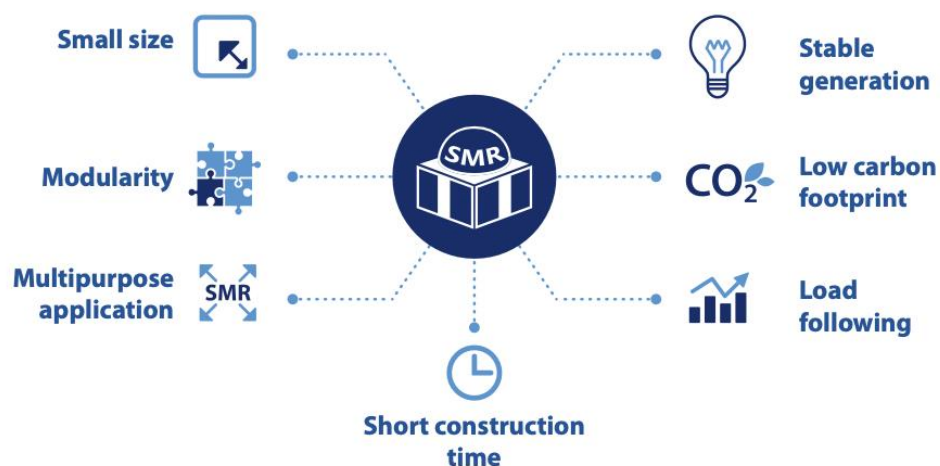


Figure 3: Advantages of SMR [4]

3 Rosatom's projects

State Atomic Energy Corporation Rosatom is one of global technological leaders, with capacities in the nuclear sector and beyond, and business partners in 50 countries. As one of the pioneers of the nuclear industry, Rosatom has traditionally been at the forefront of the international nuclear market, including nuclear power plant construction, uranium mining and enrichment, and nuclear fuel fabrication and supply.

Rosatom's business strategy is guided by the international sustainable development agenda. As a low-carbon electricity company, Rosatom significantly contributes to the achievement of the UN Sustainable Development Goals by developing nuclear, hydrogen, and wind energy. Currently, seven post-Soviet Russian-built power plants are operational in Ukraine, Iran, China, and India, with more under construction or contracted in Bangladesh, Belarus, China, Egypt, Hungary, India, Iran, and Turkey [5].

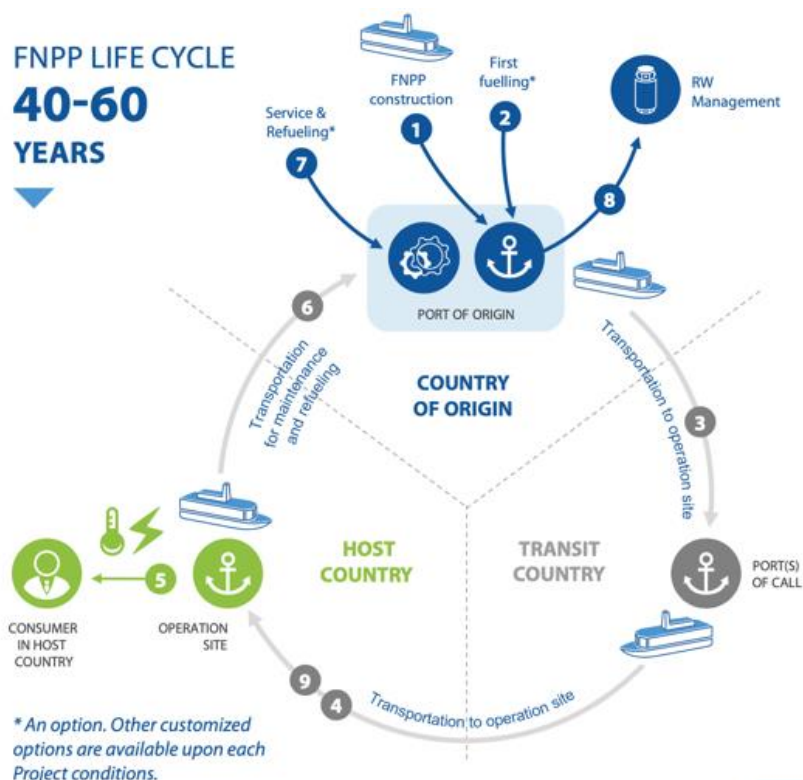
Rosatom controls all Russian Federation's nuclear assets, both civilian and military, though sometimes under various subsidiaries from operation and maintenance to nuclear waste management. [4] Therefore, Rosatom also boasts an impressive record of small reactor technology development for icebreaker fleet – about 400 reactor-years.

Rosatom is prepared to offer a flexible, tailor-made SMR solution designed to address a wide range of customer demands. Two SMR deployment options—offshore and onshore—have been developed to accommodate various climate, regional, and geographic specifics.

3.1 Offshore projects

Main function of offshore SMR is suitable for supplying electricity, heat and desalinated water to coastal areas, offshore facilities, islands and archipelagoes. [4] The lifecycle of marine based SMR is on Fig. 4. The construction process and first fueling happens in the country of origin. After transportation to operation site SMR is available for power and heat production in host country up to 10 years before refueling. In case of refueling and maintenance NPP returns to the country of origin. After maintenance it goes back to operation site.

History Soviet marine SMRs has started in the middle of XX century. There is a short historical recap of main reactors.



- | | |
|--|--|
| 1 2 FNPP construction and first fuelling in the country of origin * | 6 Return to the country of origin for maintenance and refueling |
| 3 4 Transportation to operation site through the territorial sea of transit countries | 7 Maintenance and refueling in the country of origin* |
| 5 Power and heat production at operation site in host country (up to 10 years before refueling) | 8 Radwaste management in the country of origin |
| | 9 Return to operation site |

Figure 4: Life cycle of offshore NPP [4]

3.1.1 OK-150

The first-generation reactor installation was of the loop-type OK-150 for the icebreaker Lenin with thermal power 90 MW(t). The decision to develop it was made in 1953. The reactor installation was created for the first time, without a ground-based prototype or sufficient knowledge about the operation of ship-borne reactors. Specifically, a variant in which the run time was increased by introducing a consumable absorber, using zirconium alloys instead of stainless steel as structural materials for the elements of the core, was validated [5]. The icebreaker was commissioned in 1959.

The OK-150 origination and operation experience gave variable material for subsequent improvement of future generations of ship and marine reactor installations. The main notes concerning the reactor installation according to the operational results are short life of the stainless-steel turbine system of the steam generators and plug-in corrosion-resistant jacket for protecting the case, insufficient maintainability, and high operating costs. [5]

Table 1: Characteristics of OK-150

| | |
|----------------------|-----------|
| Thermal power, MW(t) | 3x150 |
| Reactor type | Loop type |
| Design life, hours | 12000 |

3.1.2 OK-900

OK-900 is a second-generation replaced first-generation and developed for the new Arktika class icebreakers. The OK-900 design is based on other conceptual solutions. Specifically, a block arrangement, in which the pumps and steam generators are connected with the reactor by means of short “pipe in pipe” connections, was adopted for the main equipment.

The steam compensation system is replaced by a gas system. The reactor vessel is entirely welded with an elliptical bottom and internal anti-corrosion surfacing. The primary-loop coolant of the steam generator is situated in the inter-pipe space, and a specially developed titanium alloy was used instead of stainless steel for the piping system. Two reactors, whose thermal power was increased from 90 MW to 159 MW, were installed in the icebreaker. The OK-900 installation operated successfully on the nuclear icebreaker Lenin from 1970 to 1989 [6].

Table 2: Main technical characteristics of OK-900

| | |
|--|-----------------|
| Specified service life of the major equipment, h | 100 000 |
| Specified lifetime of the major equipment, years | 25 |
| The mass of two RUs within the containment, t | 2603 |
| Containment dimensions of two RUs, L × B × H, m | 7,6 x 13,3 x 20 |
| Thermal power, MW | 2x171 |
| The number of cycles of power change, thousand | 64,94 |
| The service life of the main equipment, years | 34 |
| The minimum temperature of the coolant during hydraulic tests at the end of operation, ° C | 140 |

3.1.3 KLT-40

The next stage of the development of reactor installations for civilian ships was the development of KLT-40 with thermal power 135 MW(t) for the lighter Sevmorput and KLT-40M with thermal power 171 MW(t) for the ice breakers Taimyr and Vaigach with limited draft. The reliable operation of the installations OK-900 and OK-900A made it possible to use standardized equipment on the indicated ships. In KLT-40 the protective shell was modified and a system for protecting the primary loop from over pressurization, a system for filling the shell on sinking of the ship, and other systems

were introduced for the first time [6]. KLT-40 was designed in accordance with the requirements of the IMO international safety code for commercial nuclear-powered ships. The modified variant KLT-40M has optimized biological protection of smaller mass to reduce the draft of the icebreaker, and improved systems for purification and cooldown using a heat exchanger with a recuperator [5].

Table 3: Characteristics of KLT-40M

| | |
|--|------------------|
| Thermal power, MW(t) | 2x171 |
| Reactor type | Loop type |
| Design life, hours | 50 000 – 100 000 |
| Number of RPs, units | 2 |
| Electric power, MW(e) | 2x35 |
| Time interval between refueling, years | 2.5-3 |
| Operating time, years | 40 |

3.1.4 RITM-200M (marine-based)

RITM series – is the latest development in Rosatom’s new generation SMR line and has incorporated all the best features from its predecessors [4]. Initially it was developed for icebreakers, later it was adapted for nuclear power plant design.

In contrast to the operating icebreakers with block reactor installations, a new reactor installation, the RITM-200M, was developed for general-purpose icebreakers. Its fundamental feature is an integral-type steam-generating block (Fig. 5). This design minimizes the mass and size metrics, increases the radiation resource of the vessel, allows for a core with the required energy resource, and simultaneously reduces the block dimensions. It also enhances safety in accidents, including Loss of Coolant (LOC) accidents, providing a significant advantage over the reactor installations built and designed at that time [6].

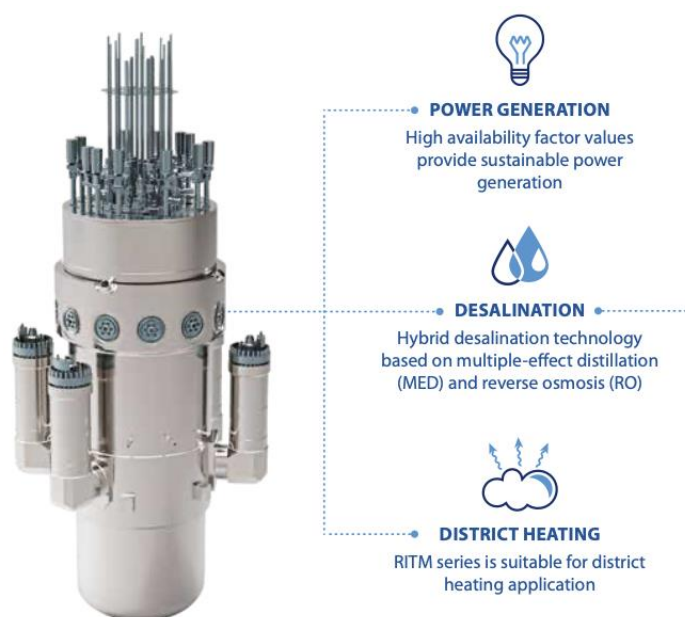


Figure 5: Steam-generation block of the RITM-200 reactor installation [4]

Table 4: Characteristics of RITM-200

| | |
|---|---------------|
| Thermal power, MW(t) | 2x175 |
| Reactor type | Integral type |
| Number of RPs, units | 2 |
| Electric power, MW(e) | 2x50 |
| Time interval between refueling, years | 10 |
| Operating time, years | 40 |
| Primary operating pressure, MPa | 15,7 |
| Primary coolant temperature: | |
| - Inlet, °C | 277 |
| - Outlet, °C | 313 |
| Primary coolant flow rate through the r.c., t/h | 3250 |
| Steam parameters: | |
| - Temperature, °C | 295 |
| - Pressure, MPa (abs.) | 3,82 |

3.1.5 RITM-400

The RITM-400 reactor installation was developed for use as the main source of energy for the nuclear turboelectric icebreaker Lider (project 10510). This icebreaker is intended for pilotage of large-tonnage vessels and leading caravans in the Arctic. The technical design initially involved a cassette zone of the type in RITM-200, but during the development work it was reoriented toward a channel core. The cassette zone allows a higher uranium content compared with a channel core, but its operating experience is

limited. The channel cores have great operating experience in transport reactors as well as higher energy density with lower flow of coolant along the first loop. The design of the FA and the elemental base of cores with a channel structure were confirmed by the long-time operation of transport reactors. [5]

Table 5: Main technical characteristics of RITM-400

| | |
|--|-------------|
| Thermal power, MW | 315 |
| Steaming capacity, t/h | 450 |
| Steam temperature, °C | 295 |
| Steam pressure, MPa | 3,8 |
| Feed water temperature, °C | 105 |
| Lifetime of replaceable equipment, years | 20 |
| Unit mass of two RUs, t | 2920 |
| Unit dimensions of two RUs, m | 9x18,2x17,5 |
| Period between refueling, years | 6 |

3.2 Onshore project

The scheme of nuclear power plant site is shown on Fig. 6. It represents a ground-based small nuclear power plant (SNPP) with two modernized reactors RITM-200 used in the universal nuclear icebreaker. A SNPP with two RITM-200 reactors is purposed for generating electricity on sites with a wide range of environmental and climatic conditions. If necessary, it can be equipped with heating and desalination facilities. [7]

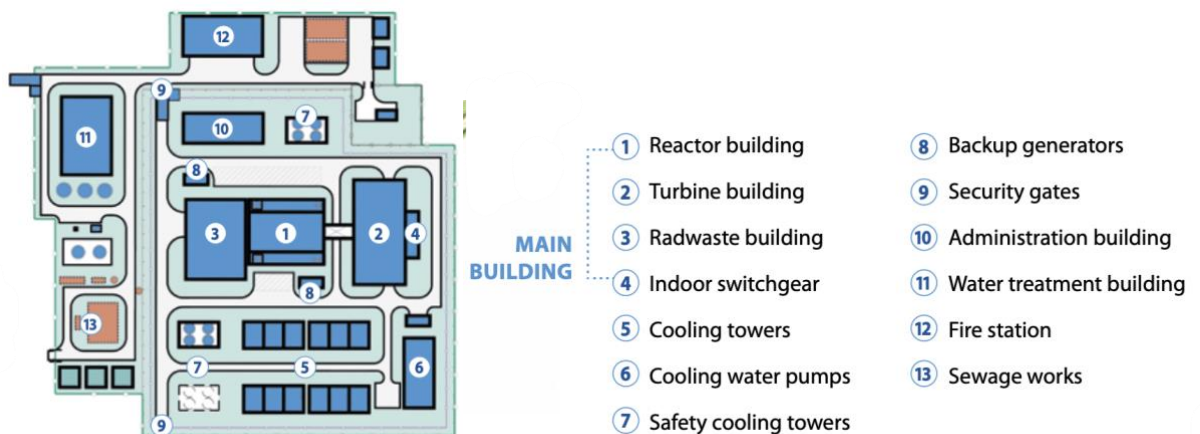


Figure 6: Layout of land-based RITM-200 [4]

The SMR includes the following buildings and structures (Fig. 6): the main block, a special block for two units, a pump station for supplying process water to the machine room, administrative and living units, and others. The basic units of the power plant are arranged in the main building: reactor, turbine, engineering systems, and handling of liquid and solid radwaste. [7]

A non-standard arrangement of the main building, compared to VVER designs, was chosen to reduce the volume of construction and assembly work and minimize technical servicing and refueling costs. Specifically, two reactor plants are arranged in the main building, with the equipment in each plant housed within an individual sealed protective shell.

Table 6: Characteristics of RITM-200

| | |
|---|------|
| Electric power on the generator terminals, MW | 2x55 |
| Time between refuelings, years | 6 |
| Time between overhauls, years | 20 |
| Service life, years | 60 |
| Approximate construction time, years | 4 |

4 Safety requirements for RITM-200

The main requirement for safety system is a desire to increase inherent safety of the system. The design of the SNPP with a RITM-200 reactor complies with modern global specifications and trends in the field of safety of nuclear power facilities. The following systems are provided for safety security in reactivity accidents [7]:

Two subsystems of electromechanical emergency shutdown:

- Emergency protection rods – release under the action of accelerating springs,
- Compensating rods – release with self-propulsion or lowering by a stepping electric motor.

Four channels are provided to cool the core in the event of depressurization of the first-loop system. Each channel functions as a safety system, accounting for a single failure: two active channels of the cooling system from makeup pumps and water tanks.

These systems ensure the reactor installation remains in a safe state during all types of accidents. For instance, in the event of the most unfavorable combination of accidents involving loss of coolant and loss of electric power, a safe state is maintained for at least three days. Serious accidents are managed by systems that fill the reactor's caisson with water to prevent vessel melt-through, reduce emergency pressure, and mitigate hydrogen combustion within the protective shell.

Several safety systems, such as the Passive Residual Heat Removal System (PRHRS) and the Safety Injection System (SIS), incorporate both active and passive functions, enhancing the inherent safety of the RITM-200. The arrangement of these systems is depicted in Fig. 7.

The PRHRS is designed to remove residual heat from the core after reactor shutdown. Active trains remove heat from the core through a steam generator and the heat exchanger of the primary circuit (5) coolant purification loop. Two passive safety loops use natural coolant circulation from (6) water tanks through steam generators, (7) air-to-water heat exchangers, and (8) water heat exchangers [4].

The SIS is designed for water injection into the primary circuit to mitigate the consequences of a Loss-of-Coolant Accident (LOCA). The system comprises two passive pressurized (9) hydraulic accumulators and two active channels with (10) water tanks and two (11) makeup pumps in each channel for redundancy.

The use of passive and self-actuating systems and safety devices is crucial for ensuring the safety of the reactor unit (RU), as it limits the adverse influence of external system failures, energy sources, and human errors. The design incorporates passive operation devices and systems that operate based on natural processes and do not require any external power.

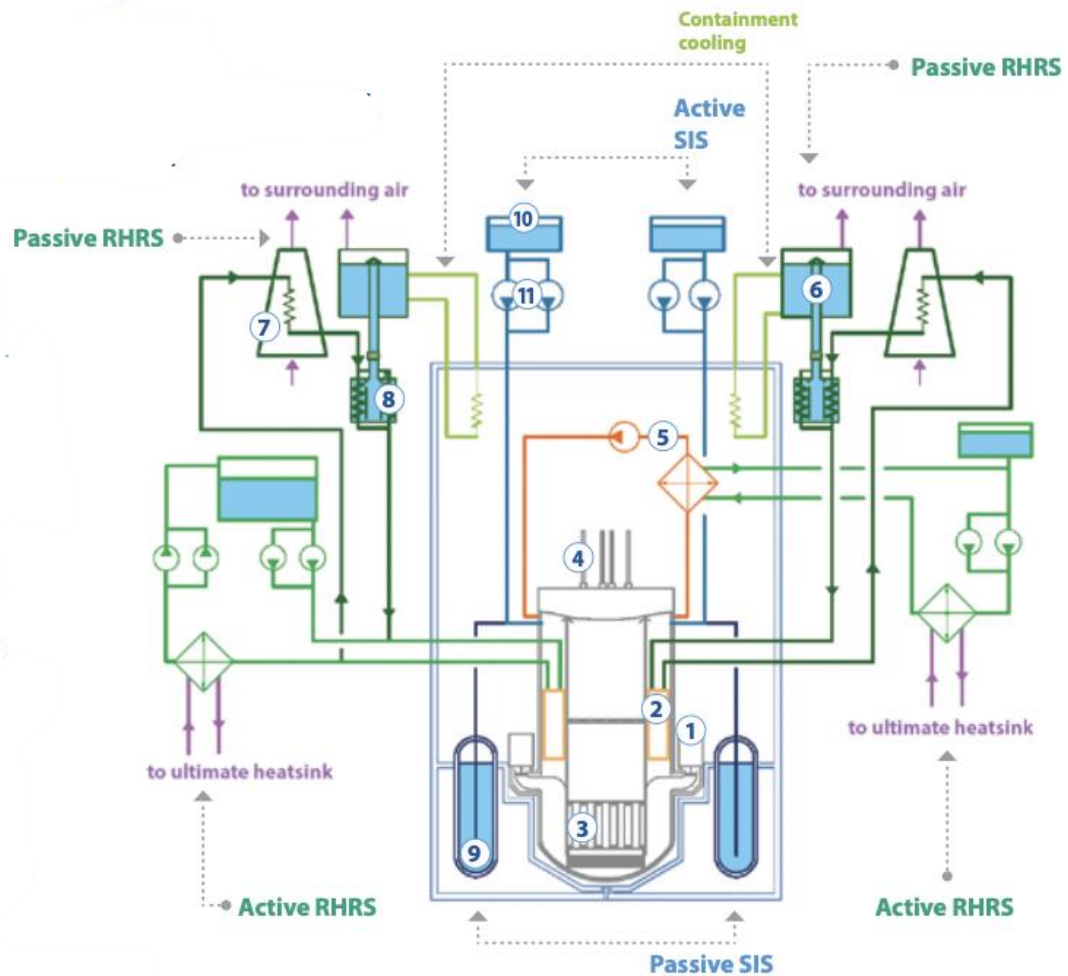


Figure 7: RHRS and SIS arrangement [4]

4.1 Passive residual heat removal system (PRHRS)

The radioactive energy emitted is known as decay heat. Therefore, heat generation still occurs in the reactor fuel, even though the NPP has been shut down by stopping the fission reaction. The power level of the decay heat is approximately 6% in comparison with nominal power. [8]

Passive residual heat removal system also known as PRHRS and two active channels are incorporated into the design. A distinctive feature of this design is the inclusion of an air heat exchanger in the passive ECS channel, in addition to a water heat exchanger (Fig. 8). The passive ECS is implemented as two independent channels, each capable of cooling the reactor installation from residual power level using natural circulation of the coolant in the loops indefinitely, as long as the primary loop remains hermetically sealed. In accidents involving depressurization, it extends the safe state time margin.

The power of the air heat exchanger is selected so that, by the time the stored water in the cistern is exhausted, the residual heat release can be removed without relying on the water heat exchanger [5].

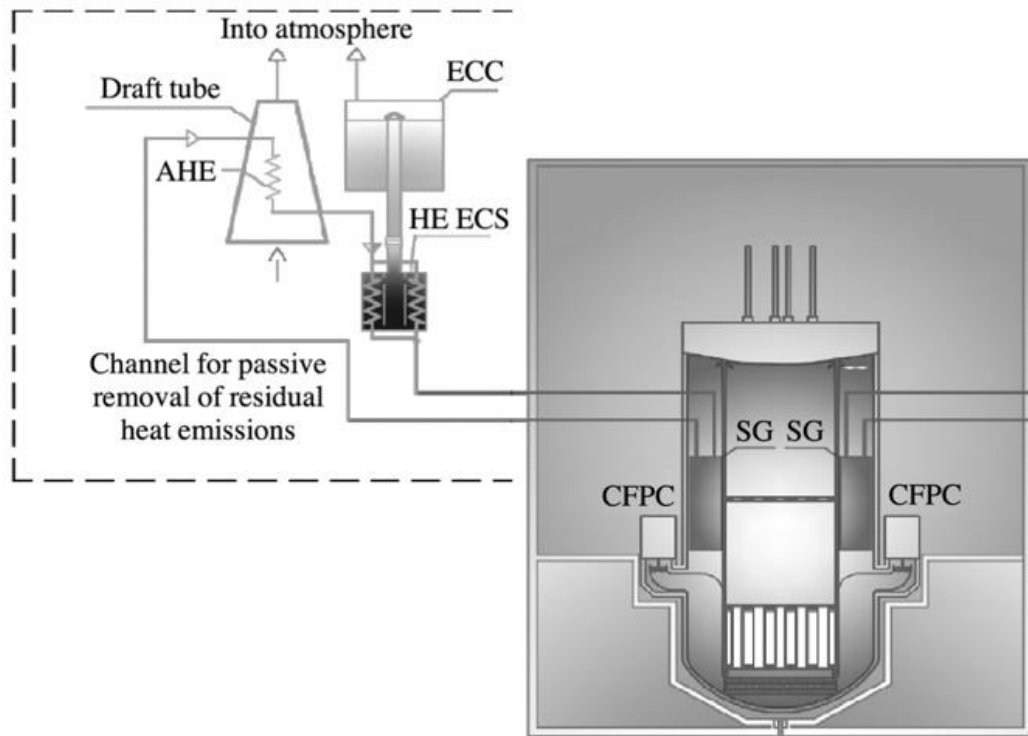


Figure 8: Schematic diagram of the passive residual heat removal system in RITM-200 [5]

5 Description of components of RITM-200

As the analysis shows, trying to improve one characteristic of equipment it may have opposing effects on the other parameters of the installation. Therefore, the developers have found compromise solutions to ensure the best possible results for RITM-200. When selecting the core parameters, it was considered that an increase in the outlet temperature, on one hand, improves the quality of steam and the efficiency of the cycle, and reduces the heat exchange surface of the steam generator. On the other hand, it decreases the resource capacity of core elements made of chromium-nickel and the pipe system of steam generators made of titanium alloy. A similar example is related to the flow rate of the primary coolant. Its increase improves the thermal engineering conditions (e. g. improved heat exchanger efficiency) of the equipment but also leads to an increase in pump power.

Therefore, the designers considered it advisable to accept the parameters of the core of the RITM-200 reactor plant as close as possible to the parameters of the VVER. This was facilitated by a significant decrease in energy intensity, the temperature of the coolant at the outlet of the core, an increase in pressure in the primary circuit, and an increase in flow compared to current analogues. Nevertheless, the use of progressive design solutions in the RITM-200 project, even with reduced thermal loads, made it possible to obtain the minimum dimensions and weight for such a power, combined with high safety, and to ensure acceptable technical and economic indicators (see the table 7). [9]

Table 7: General characteristics of reactor unit (RU)

| | |
|---|---------------------|
| Primary operating pressure, <i>MPa</i> | 15,7 |
| Coolant inlet temperature, °C | 277 |
| Coolant outlet temperature, °C | 313 |
| Coolant flow rate through reactor core, <i>t/h</i> | 3250 |
| Streaming capacity, <i>t/h</i> | 248 |
| Steam temperature, °C | 295 |
| Steam pressure, <i>MPa</i> | 3,42 |
| Neutron fluence at the end of lifetime, <i>N/cm²</i> | $5,2 \cdot 10^{19}$ |
| Electric power, <i>MW</i> | 2 x 55 |
| Time between refueling, <i>years</i> | Up to 6 |
| Approximate construction time, <i>years</i> | 4 |

The nuclear power unit (NPU) has two reactor units based on an integrated type of water-moderated reactor with a thermal capacity of 175 MW, located in individual containment shells. Steam (248t/h) from each RU is generated according to a two-circuit scheme, which has been traditionally worked out in nuclear power engineering by transferring heat from the primary circuit to feed water and to a second circuit steam in the steam generator (Fig. 9). Reducing the neutron fluence on the case allows to increase the radiation durability of the steam generation unit case and reduce the temperature during hydraulic pressure tests. [10]

The safety control of RITM-200 RU is based on the following principles: high heat-storage capacity, natural circulation of the primary coolant, sufficient for the reactor shut-down cooling, the minimum length of the primary pipelines, the use of outflow restrictors in small pipe branches, a larger volume of the primary coolant in the reactor shell compared to the block design. All this increases the time slack until the core section is drained in accidents with a primary coolant leak.

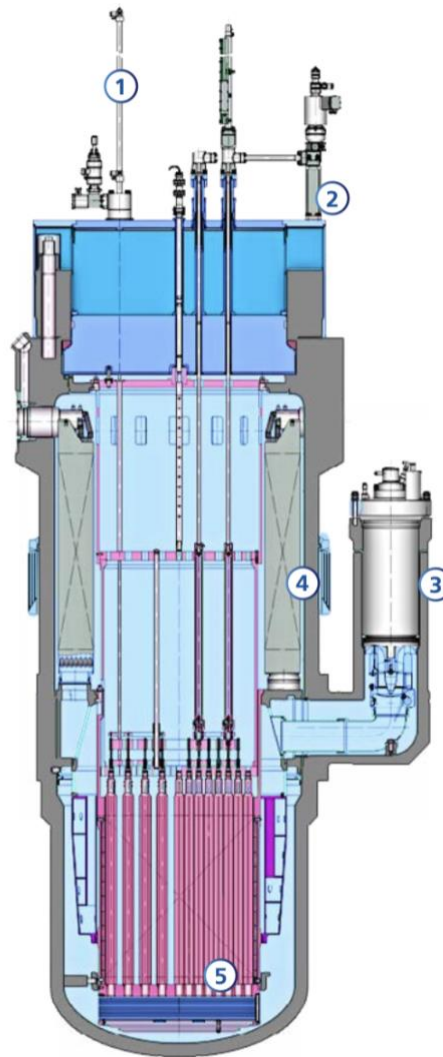


Figure 9: RU general view [10]

1 - group of emergency protection actuators, 2 - group of executive mechanisms compensating for reactivity, 3 - primary central pumps, 4 – steam generator, 5 – reactor core.

5.1 Reactor unit (RU)

The design of the RITM-200 reactor unit is based on integrated type SGU with forced circulation, the steam generator cassettes (SG) are located inside the case, the primary central pumps (PCP) in separate remote hydraulic chambers, and the reactor core with increased energy source. This type of SGU is defined by greater compactability compared to block type SGU used on active nuclear-powered ships, where steam generators are located in separate cases. [7]

The compactability of the steam generation unit allows to reduce the weight and dimensions, which cuts down the volume and duration of installation work directly at the shipyard, as well as improves the manufacturing quality of the steam generation unit due to the completion of all works under the machine-building plant conditions. At the same time, the disposal of the unit is simplified due to the possible unloading of the entire steam generation unit with a minimum amount of disassembly.

The main circulation path of the primary circuit heater is located in the steam generating unit. Such a constructive execution of the unit has increased reliability in terms of reducing the number of large-diameter pipes and equipment housings under pressure of the primary circuit, while maintaining high manufacturability and acceptable maintainability. The hydraulic resistance of the circulation circuit was significantly reduced, which made it possible to increase the flow, reduce the power of the pumps and ensure a high level of natural circulation. The integrated design of the steam generating unit made it possible to place a large-sized active zone in it, while ensuring minimal weight and dimensions, as well as the possibility of transportation by rail. The manufacture of all body elements using the currently adopted technology is carried out without modernization of production. [9]

The steam-generating unit is intended for producing superheated steam. It is formed based on a water-moderated and cooled reactor with forced circulation of first-loop coolant and a remote gas-pressure equalization system. Its vessel contains the core, four steam generators, and the main elements of the coolant-circulation channel. In addition, four water tanks with pumps installed are located on the lateral surface of the vessel. Twelve drives of the equalization groups and six drives of the emergency protection are installed on the unit's lid. [7]

Safety of reactor core is carried out by protection control system drives (CPS). First group of drives is group of emergency protection actuators. They are needed to quickly shut down the reactor and maintain it in a subcritical state in an emergency. Second group of drives is group of executive mechanisms compensating for reactivity. It is designed to compensate for excess reactivity power in the start-up, power operation and shutdown modes of the reactor.

Amount of each component of RU are mentioned in Table 8.

Table 8: Amount of RU's components

| | |
|---|----|
| Reactor core | 1 |
| PCP | 4 |
| Steam generator | 4 |
| Group of emergency protection actuators | 12 |
| Group of executive mechanisms compensating for reactivity | 6 |

5.2 Reactor core

Neutrons are moderated by the demineralized water contained in the pressure vessel. The specific composition of the low-enriched (14 %) Dioxide Uranium (UO_2) fuel has a large prompt negative thermal coefficient of reactivity. This means that, as the temperature of the core increases, the reactivity undergoes a prompt decrease [11]. Density of fuel is 10600 kg/m^3 .

The design used a cassette-type reactor core with cermet fuel of increased uranium intensity, which, unlike intermetallic fuel, meets the requirements of non-proliferation of nuclear arms. Main technical parameters of reactor core are in Table 9. A cassette-type core is used in the reactor installation. The core consists of a complex of FA, startup sources of neutrons, emergency protection rods and barrel sleeves for thermometers, emergency protection rods, neutron sources, and detectors for neutronics monitoring. [7]

Table 9: Parameters of reactor core

| | |
|--|----------------------------------|
| Service life, h | 75 000 |
| Lifetime, years | 12 |
| Height of the core, mm | 1200 |
| Diameter of the core, mm | 1500 |
| FA spacing, mm | 101 |
| Core volume, m^3 | 2,9 |
| Fuel rod type | Cylindrical E-635 alloy cladding |
| Fuel composition | UO_2 + silumin |
| Power capacity, $TW \cdot h/m^3$ | 2,13 |
| Number of fuel assemblies | 199 |
| U-235 core charge, kg | 438 |
| Enrichment, % | 14,06 |
| U-235 specific consumption, $g/MW \cdot day$ | 2,3 |
| Inner diameter of fuel rod, mm | 5,9 |
| Outer diameter of fuel rod, mm | 6,9 |

The core contains 199 fuel assemblies. According to [12] the structure of the fuel assembly remained the same as in KLT-40 reactor. Each assembly has 69 fuel rods, 9 burnable type-one absorber rods and 6 type-two absorber rods, and 7 control rods in the center of the fuel assembly (Fig. 11). Burnable type-one and type-two absorber rods are distinguished by the density of burnable absorber [15]: in type-one rod gadolinium density equals 2.7 g/cm^3 , whereas in type-two rod gadolinium density equals 1.4 g/cm^3 . Structurally, the fuel rod is a smooth rod with a diameter of 6.9 mm with a length of the fuel containing part of 1200 mm. Zirconium alloy E-635 (98% Zr, 1% Nb, 0.8% Sn, etc.) is used as fuel cladding, because it has a higher corrosion resistance and resistance to disruption of the water chemistry regime than the traditional zirconium alloy E110. The thickness of the cladding is 0.5 mm.

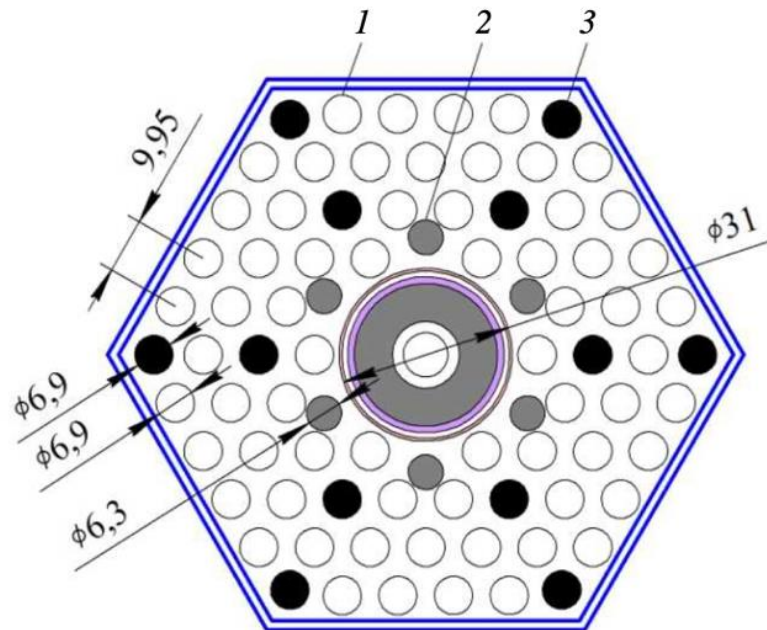


Figure 10: Fuel assembly of RITM-200 [15]:

1 — fuel rods; 2, 3 — rods of the exhaust absorber.

Changes have been made to the cores of III+ generation reactors to enhance their reliability, including a decrease in specific energy release and maximum heat flux density in the core. The reduction in specific energy release is achieved by either lowering the nominal power of the core or increasing the volume of the core. [13]

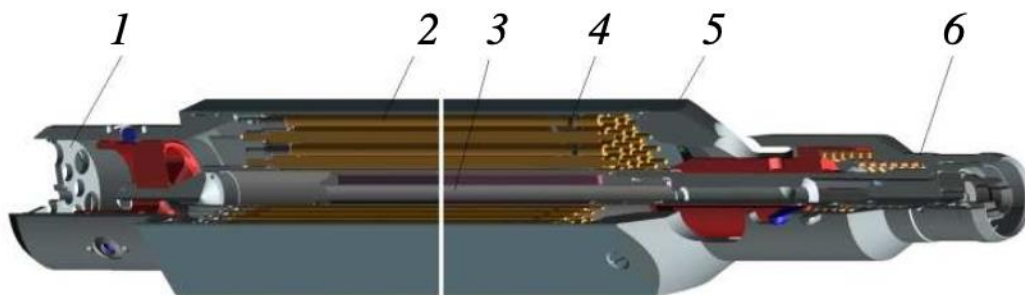


Figure 11: General view of the fuel assembly [15]:

1 — calibration washer; 2 — fuel rod, core of the burnout absorber; 3 — absorbing element; 4 — spacing grid; 5 — cover; 6 — head

The fuel assembly includes, in addition to fuel rods, a set of elements that compensate for reactivity (Fig. 10). In the bundle of 91 elements, 19 fuel rods are excluded: seven fuel rods for placing a central displacer with an absorbing element, six fuel rods near the central displacer and six angular fuel rods to ensure reliability requirements, i.e., the fuel assembly can contain no more than 72 fuel rods. [14]

5.3 Steam generator

The reactor plant uses a highly efficient direct-flow straight-tube steam generator, the specific steam capacity of which is more than 2 times higher than the operating coil ones.

The configuration of the steam generating cassettes ensures their compact placement in the housing of the steam generating unit. Compared with the analog, the nodes in the new steam generator have been changed or eliminated, which create conditions for a local increase in the concentration of hydrogen, contributing to hydrogenation and failure of the pipe system during operation. [9]

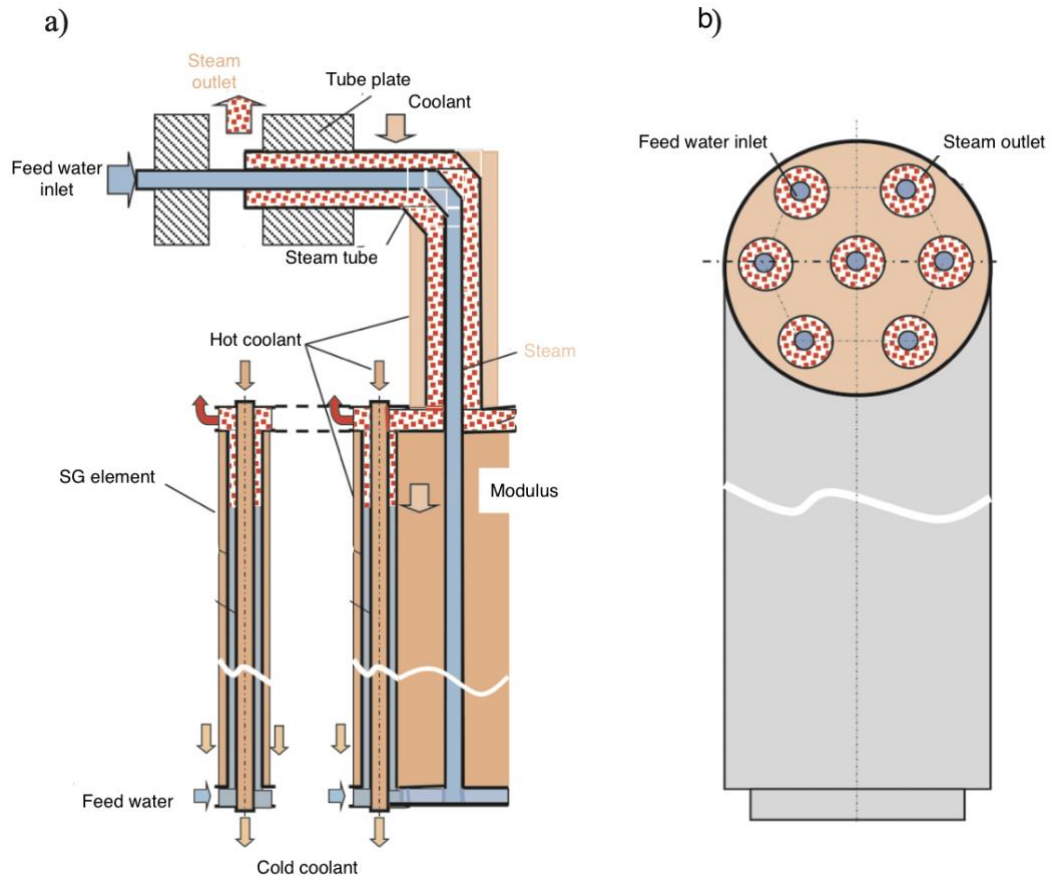


Figure 12: Scheme of the steam generating cassette of the steam generator RU "RITM-200M" [9]:
 a — diagram of the flow directions of the working fluid and coolant; b — view of the cassette from the feed water inlet and steam outlet

In RU with an integrated layout, the most acceptable is the formation of a pipe system in the form of straight tubes — a set of steam generating elements (SGE) grouped into modules with a parallel collector connection for feed water and steam. The modules are the minimum shut-off surface during repair. At the same time, each module has its own supply of feed water and discharge of generated steam, as well as access to them to mute individual modules. For ease of assembly, the modules are combined into cassettes placed between the reactor vessel and the internal shaft. SGE consists of two tubes of different diameters, between which an annular channel is formed, into which the feed water enters. As a result, two-way heating of the feed water is carried out with a coolant passing outside the outer tube and in the inner tube. Figure 12 shows the diagram of the steam generating cassette of the icebreaker's RITM-200M. The table 10 shows the main design and energy characteristics of integrated steam generators [15].

At the same time, the feed water inlet (temperature 105 °C) was combined with the steam outlet from the cassette (temperature about 300 °C) and heat exchange was provided between them. As a result, a kind of heat exchanger (a "pseudo-regenerative" section) was formed, where the temperature of the steam coming out of the module decreases the more the lower the reactor power. As a result, the effect of reducing underheating in the superheating section in nominal and variable modes is disavowed by cooling in the "pseudo-regenerative" section. [15]

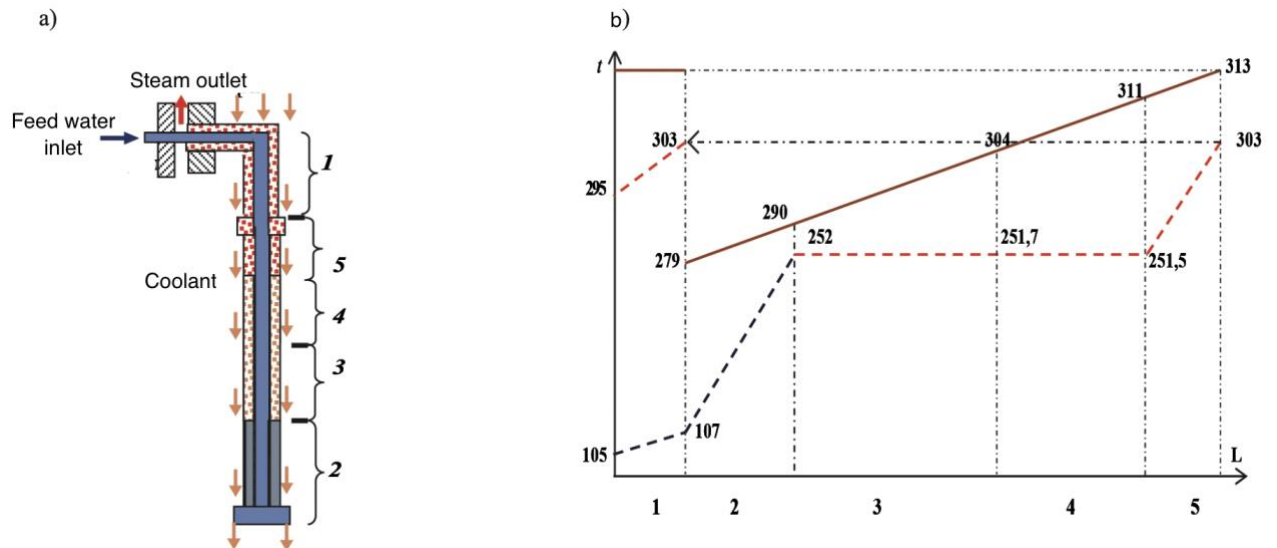


Figure 13: Scheme of feed water supply and steam removal from the module (a), calculated values of coolant and steam temperatures along the path of media movement in the cassette for the nominal feed water flow rate [15].

Symbols:

- 1 – steam cooling section in the central supply (feed water inlet – steam outlet) – "pseudo-regenerative" section;
- 2 – economizer section along the inner surface of the primary circuit of the SGE.
- 3 – the evaporation section located below the overflow holes of the cassette; 4 – the evaporation section located above the overflow holes of the cassette.
- 5 – superheating section on the side of the primary circuit of the inner cavity of the SGE

Temperature distribution of the working fluid and coolant over the phase sections of heat exchange and at the outlet of the cassettes at the nominal operating mode of the control unit are on Figure 13. The design decisions taken to place the feedwater inlet pipes inside the steam outlet pipes led to the formation of a "pseudo-regenerative" area where the steam temperature decreases due to the cooling of the incoming feedwater. Fig. 13,a shows the scheme of feedwater supply and steam removal from the module. [15]

Fig. 13, b shows the calculated values of the temperatures of the coolant and steam along the path of media movement in the cassette for the nominal flow rate of feed water. At the outlet of the superheating section, the steam temperature is 303 °C. However, after passing through the "pseudo—regenerative" section, the steam temperature decreases to

295 °C. In this case, the heat transfer process involves a coolant washing the steam pipe, steam coming out of the pipe, and feed water entering the cassette. [15]

Table 10: Main design characteristics of steam generator

| Name of the value | Cassette | Section |
|--|-------------------|---------|
| Transverse size of heat exchange pipes, mm | 13 x 1,5; 8 x 1,5 | |
| Number of cassettes per section | 3 | - |
| The number of moduli | 7 | 21 |
| Number of heat exchange tubes in modulus per section | 118 | |
| Number of heat exchange tubes | 826 | 2478 |
| Heat exchange tube material | PT-7M Alloy | |
| Heat exchange surface, m ² | 93,4 | 280 |
| Thermal power, MW | 14,5 | 43,7 |
| Steam capacity, kg/s | 5,74 | 17,22 |

Weakly superheated steam is traditionally used in transport engines, which makes it possible to reduce the final moisture content of steam with a single-body turbine design. This solution reduces the achievable efficiency of a steam turbine installation compared to the possible efficiency when using saturated steam with a similar temperature (increased pressure). It should be noted that an increase in the pressure of the generated steam at a constant temperature leads to an increase in its final humidity. The use of intermittent inter-body moisture separation in the steam turbine cycle will avoid increased final humidity. This solution creates a certain margin for increasing the steam parameters in a steam turbine installation. [13]

Titanium alloy PT-7M is used as the structural material for block-section headers and section of feed water tubes and steam tubes welded to them.

Considering the difficulty of replacing the failed steam generator cassettes located inside the body of the steam generating unit, measures have been taken to increase its survivability. The pipe system is made partitioned with the possibility of disconnecting sections that have lost their tightness without removing the cover of the main connector, a significant reserve is laid on the heat exchange surface, it is possible to increase steam production by increasing the temperature of the coolant at the outlet of the core. The adopted design solutions ensure nominal steam capacity until the replacement of the steam generator cassettes during the average repair of the reactor plant.

5.4 Pump

The primary circulation loop consisted of a rotodynamic, single-stage vertical-design pump with an axially mounted cantilevered wheel and hermetic asynchronous single-winding electric motor with a dry screened stator. The pump provides two speeds for the rotor of the electric motor: 3000 and 1000 rpm. The rotational frequency can be

changed by converting the frequency of the supply current in the pump-control apparatus. [7]

5.5 CPS drives

The group of protection system (PS) actuators is designed to quickly shut down the reactor and maintain it in a subcritical state in an emergency. The group of compensating groups (CG) actuators is designed to compensate the excess reactivity in the start mode, power operation and shutdown of the reactor. The CPS RITM- 200 RU drives are based on the drives used in the KLT-40 RU.

5.6 Pressurizer

In RITM-200 reactor unit, a gas pressure compensation system (CS) is used, which allows for acceptable maneuverability characteristics and a high degree of readiness of the ship's nuclear power plant for operation compared with a steam pressure compensation system. [15]

5.7 Turbine

RITM-200 includes a steam turbine with automatic regulation, monitoring and control devices, a condenser with receiving-discharge device, equipment of the vacuum system and a system of turbine seals, and intermediate steam-separation system equipment. The turbine operates on superheated steam in the block with the reactor.

The steam turbine is intended for operating a turbogenerator in the steam-turbine installation. The turbine supplied by the Kaluga Turbine Plant is a single-cylinder assembly with intermediate steam separation and consists of oppositely directed high- and low-pressure parts. [7]

The use of intermediate moisture separation also slightly increases the efficiency and reliability of the turbine but has a negative effect on its maneuverability characteristics due to the introduction of additional energy storage volumes.

Table 11: The main technical characteristics of the K-50-3,4/50 turbine

| Design scheme | High pressure part + steam separator + low pressure part |
|---|--|
| Rotational speed | 3000 |
| Pressure of fresh steam in front of the stopped valves, MPa | 3.4 |
| Temperature of fresh steam in front of the stopped valves, °C | 295 |
| Regeneration system of steam turbine plant | 1 low-pressure heaters + deaerator + 1 high pressure heaters |
| Type of feed pump drive | Electric drive |
| Number of regenerative samplings | 3 |

6 Modeling of RITM-200 system

The aim of this work is to investigate the conceptual design of a ground-based small nuclear power plant (SNPP) featuring two modernized RITM-200 reactors, originally used in universal nuclear icebreakers. The primary objective is to illustrate the "load following" capability of the reactor. The second goal is to perform a dynamic analysis of the Passive Residual Heat Removal System (PRHRS) in the event of full control rod insertion. The modeling is performed using the Dymola simulation environment.

Modelica is a unified modeling language designed for complex physical systems incorporating multidisciplinary components. As an equation-based modeling language utilizing differential algebraic equation solvers, it allows users to focus on the physics of the problem rather than the solving methodology. This results in faster model creation and analysis. This feature, along with its system flexibility, has propelled the Modelica language into widespread use across various industries, including automotive, aviation, aerospace, and satellite constellations. [16]

Modelica language offers an object-oriented approach that makes the modeling of complex systems flexible, modular and re-usable. Components are based on non-linear, first-principles models and are either lumped-parameter models or 1-D distributed parameter models. [11]

The model of the RITM-200 plant has been built using component models from ThermoPower Modelica library. The ThermoPower library is open-source and has been developed for the modeling of thermal power plants at system level. Models are derived from first principal equations whenever possible, e.g. mass, momentum, and energy dynamic balance equations, or from acknowledged empirical correlations.

The Modelica model of the small light-water reactor system was established, as illustrated in Figure 15. The model comprises 3 subsystems with data exchange facilitated by the Modelica interface and model for PRHRS which will be explained later. The tree subsystems and PRHRS are described as follows.

- Reactor system. The core heat is generated by the reactor system serves as the energy source. The system includes point kinetics, decay heat power, and thermal-hydraulic models.
- Steam generator. This system describes heat transfer from coolant to feed water in a vertical straight-tube heat exchanger consisting of cassettes and modulus.
- Secondary side system focuses on the Rankine cycle to facilitate heat-work conversion. The system encompasses models of turbines, separator, regenerative heaters, and deaerator.
- Safety system. Passive residual heat removal system consists of models of air heat exchanger and water heat exchanger connected with emergency core cooling (ECD) water tank.

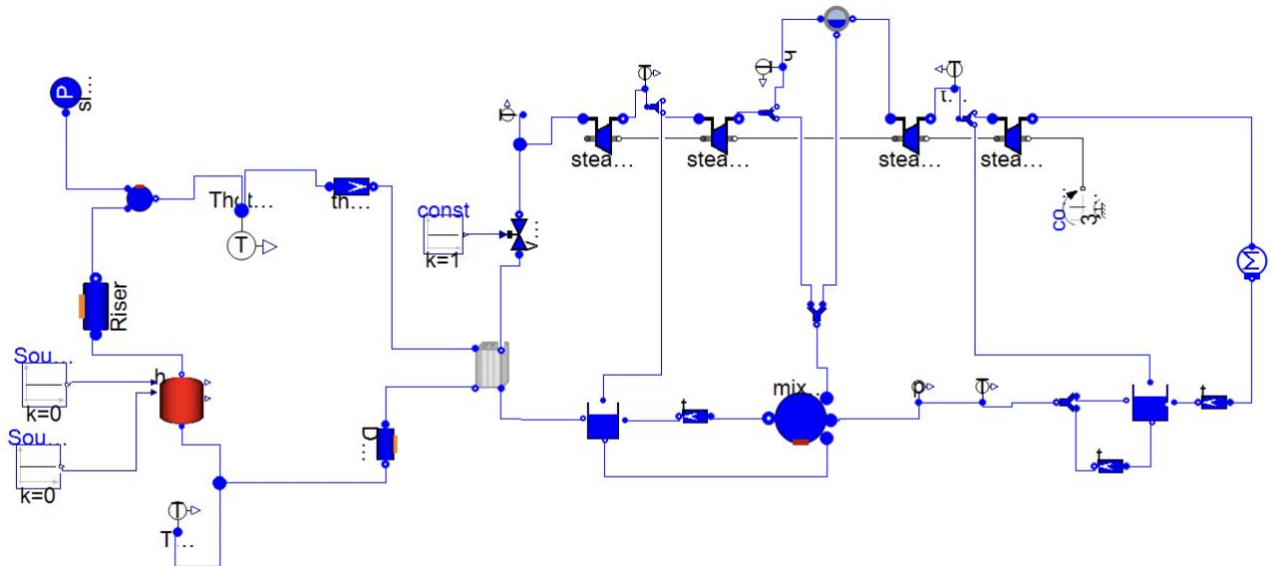


Figure 14: Model of RITM-200

It is important to mention that some mass-through components from the Thermopower library have been used to drive forced circulation in the two circuits. These components, together with pressure sinks, allow to avoid the usage of pumps for the sake of simplification due to lack of information about pump's characteristics.

6.1 Reactor core

The Modelica model of the reactor system is depicted in Figure 16, encompassing point kinetics, thermal, and hydraulic models. The inlet and outlet of the coolant within the reactor system are connected to the downcomer and riser, respectively. This model was created by master's students in previous years. I have made several modifications to enhance its accuracy and functionality.

These modifications include incorporating the dependence of thermal power on neutron flux and describing the reactivity impact of poisons using equations for the concentrations of xenon and iodine. Additionally, I implemented the decay power law into the model.

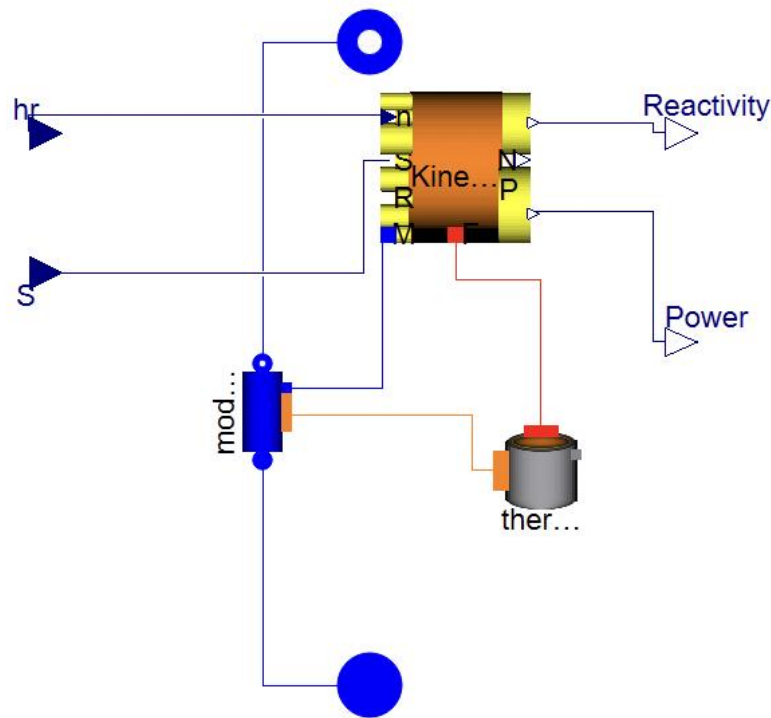


Figure 15: Model of reactor system.

6.1.1 Neutronics

The neutronics has been described adopting a point reactor kinetics model, with one energy group and six delayed neutron precursors groups: this approximation consists in grouping together the precursors based on their half-lives. Delayed neutrons are represented by six groups: yields (neutrons per fission) and decay constants (λ , sec^{-1}) are obtained from nonlinear least-squares fitting to experimental measurements. [11]

The reactor neutron model is based on point reactor neutron dynamics. The three-dimensional (3-D) effect of neutron space dynamics is neglected, with the neutron flux distribution fixed in space and varying only with time. The equations are listed as follows [17]:

$$\frac{dN}{dt} = \frac{\rho - \beta}{\Lambda} N + \sum_{i=1}^6 \lambda_i C_i \quad (6.1)$$

$$\frac{dC_i}{dt} = \frac{\beta_i}{\Lambda} N - \lambda_i C_i, i = 1, \dots, 6 \quad (6.2)$$

$$\beta = \sum_{i=1}^6 \beta_i \quad (6.3)$$

$$\rho = \rho_{init} + \rho_{fuel} + \rho_{Xe} + \rho_{CR} + \rho_{coolant} \quad (6.4)$$

$$\rho_{fuel} = \alpha_f (\Delta T^{fuel}) \quad (6.5)$$

$$\rho_{coolant} = \alpha_c (\Delta T^{coolant}) \quad (6.6)$$

Here, N represents the average neutron density, Λ denotes the neutron generation time, β signifies the total delayed neutron fraction, β_i indicates the delayed neutron fraction of group $[i]$, C_i is the precursor concentration of the delayed neutron of group $[i]$, λ_i is the decay constant of the delayed neutron of group $[i]$, and ρ stands for the net reactivity. The initial reactivity (ρ_{init}), xenon reactivity (ρ_{Xe}), and control rod reactivity (ρ_{CR}) introduced by inserting or exerting control rods.

The Doppler Effect, affecting on fuel reactivity (ρ_{fuel}), in nuclear physics refers to the broadening of resonance absorption peaks in fuel isotopes (especially U-238) as fuel temperature increases. This effect plays a crucial role in reactor stability by providing negative feedback to fuel reactivity α_f . A negative fuel feedback coefficient is crucial for reactor stability because it provides passive safety. When fuel temperature increases, the resonance absorption of neutrons increases, reducing reactivity and slowing down the reaction. [17] It improves inherent safety of the reactor, while a reactor with positive α_f is inherently unstable. The light water reactor (LWR) core in this conceptual design possesses a substantially negative fuel temperature coefficient, roughly around -2 pcm/ $^{\circ}$ C. As for the coolant density feedback coefficient, this value is equal to -10 pcm/ $^{\circ}$ C.

Xenon-135 is a product of U-235 fission and has a very large neutron capture cross-section, which introduce negative reactivity ρ_{Xe} . It decays radioactively with a half-life of 9.1 hours. Little Xe-135 results directly from fission, but most comes from the decay chain, Te-135 to I-135 (β -decay, 6.6 hours) to Xenon-135. The instantaneous production rate of xenon-135 is dependent on the iodine-135 concentration and, therefore, on the neutron flux history. On the other hand, the destruction rate of Xenon-135 is dependent on the instantaneous local neutron flux.

$$\frac{dN_I(t)}{dt} = \gamma_I \Sigma_f \phi - \lambda_I N_I(t) \quad (6.7)$$

$$\frac{dN_{Xe}(t)}{dt} = \gamma_{Xe} \Sigma_f \phi + \lambda_I N_I(t) - (\lambda_{Xe} + \sigma_a^{Xe} \phi) N_{Xe}(t) \quad (6.8)$$

$$N_I(\infty) = \frac{\gamma_I \Sigma_f \phi_0}{\lambda_I} \quad (6.9)$$

$$N_{Xe}(\infty) = \frac{(\gamma_I + \gamma_{Xe}) \Sigma_f \phi_0}{\lambda_{Xe} + \sigma_a^{Xe} \phi_0} \gamma_{Xe} \quad (6.10)$$

$$\rho_{Xe} = \frac{-10^{-24} \cdot \sigma_a^{Xe} N_{Xe} C_t}{\nu \Sigma_f} \quad (6.11)$$

In the formulas, N_I and N_{Xe} represent the concentrations of I-131 and Xe-135, respectively. γ_I and γ_{Xe} are the yields of I and Xe per fission event, f is the macroscopic fission cross-section of the reactor core, λ_I and λ_{Xe} are the decay constants of I and Xe, respectively, σ_a^{Xe} is the microscopic capture cross-section of Xe, and ϕ is the neutron flux. C_t is the reactivity adjustment factor and is the average number of neutrons produced per fission event.

From a mathematical perspective, the equations for the point reactor are Differential-Algebraic Equations. These can be readily represented using the Modelica language. As

result, point kinetics calculates values for reactivity and generated power by nuclear fission. Radius ($2,7 \cdot 10^{-3} \text{m}$) and height (1,2 m) of fuel rod was taken from literature. [14]

6.1.2 Thermal modelling

It is the model for the heat generation in the fuel considers the radial heat transfer, neglecting both the axial and the circumferential diffusions. Five zones (Figure 17) are identified and modeled: three concentric zones in the fuel pellet with equal volume, the gap, and the cladding.

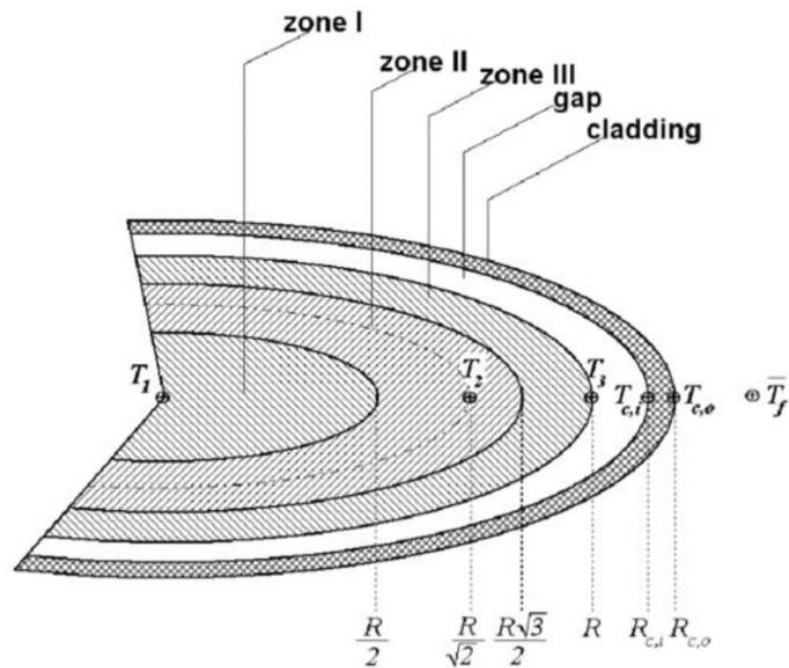


Figure 16: Radial heat transfer modelling [11]

The time-dependent Fourier equation in one-dimensional cylindrical geometry in homogeneous material is applied to each of these zones. General representation of heat conduction equation:

$$\rho c_p \frac{\partial T}{\partial t} = \frac{1}{r} \frac{\partial}{\partial r} k r \frac{\partial T}{\partial r} + q''' \quad (6.12)$$

Where ρ is the density of material, c_p is the specific heat capacity of material, k is conductivity, q''' is a specific power conducted through the volume. After double integration of this equation five equation of energy balance for each zone are obtained.

Zone I:

$$\rho_1 c_{p1} \frac{\partial T_{f1}}{\partial t} \frac{R^2}{8} = k_1 (T_{f2} - T_{f1}) + \frac{R^2}{8} q''' \quad (6.13)$$

Zone II:

$$\rho_2 c_{p2} \frac{\partial T_{f2}}{\partial t} \frac{R^2}{4} = 3 \cdot k_2 (T_{f3} - T_{f2}) + k_1 (T_{f2} - T_{f1}) + \frac{R^2}{4} q''' \quad (6.14)$$

Zone III:

$$\rho_3 c_{p3} \frac{\partial T_{f3}}{\partial t} \frac{R^2}{8} = -R \cdot h_{gap}(T_{f3} - T_{ci}) - 3 \cdot k_2(T_{f3} - T_{f2}) + \frac{R^2}{4} q'' \quad (6.15)$$

Zone IV:

$$\frac{k_c(T_{ci} - T_{ce})}{\ln\left(\frac{R_{ci}}{R_{ce}}\right)} + R \cdot h_{gap}(T_{f3} - T_{ci}) = 0 \quad (6.16)$$

Zone V:

$$\rho_{ci} \cdot c_p^{clad} \frac{\partial T_{ce}}{\partial t} \frac{R_{ce}^2 - R_{ci}^2}{2} = -\frac{k_c(T_{ci} - T_{ce})}{\ln\left(\frac{R_{ci}}{R_{ce}}\right)} + \frac{Q}{2h\pi} \quad (6.17)$$

The conditions of heat flux vanishing at the pellet center and the continuity of the temperatures and heat fluxes at the three boundaries regions allow the determination of temperatures. Average fuel rod temperature for the Doppler feedback computation (T_{act}) is calculated as follows like function of boundary temperatures:

$$T_{act} = 4/9T_{r=0} + 5/9T_{r=R} \quad (6.18)$$

where $r=0$ and $r=R$ are the center and the boundary of the fuel rod respectively.

Specific heat capacity c_p is calculated using Fink–Touloukian correlation [23] and conductivity k [24] of fuel is expressed like functions of fuel's temperature:

$$c_p = 4,186 \cdot 10^{-2}(710 + 0,6 \cdot T - 146 \cdot T^{-2} + 4\left(\frac{T}{1000}\right)^7)$$

$$k = \frac{100}{11,8 + 0,0238 \cdot T} + 8,775 \cdot 10^{-15}T^3 \quad (6.19)$$

Heat transfer coefficient (h_{gap}) of the gap is assumed like a constant value equal to $1593,77 \frac{W}{m^2K}$ and calculated as a ratio of filling gas conductivity (k_{gap}) and effective thickness of the gap (δ_{gap}), which is equal to $0,2 \text{ mm}$. Irradiation effect on gap heat transfer coefficient is neglected since it much less in comparison with conductivity value. It was assumed that filling gas is Helium, therefore certain correlations are used:

$$h_{gap} = \frac{k_{gap}}{\delta_{gap}} \quad (6.19)$$

$$k_{gap} = 15.8 \cdot 10^{-4} \cdot T[K] \quad (6.20)$$

6.1.3 Hydraulic model of coolant

Inside the core model, a 1-D tube model for water/steam flow is used, to represent the thermo-hydraulic of single-phase coolant, with a turbulent friction model for the pressure drop calculation.

Finite Volume Method (FVM), for water/steam flow in a tube, have been used to build the hydraulics circuits, one-phase, with mass, momentum, and energy balance partial differential equations. The FVM approach is a numerical technique used to solve partial

differential equations (PDEs) that arise in various fields such as fluid dynamics, heat transfer, and structural analysis.

The moderator flow passes through 13731 channels having 1.2 m length (as the active length of the fuel rods). The shape of channels is triangular (Fig. 10), therefore cross section area of the coolant flow is a function of pitch and external radius of cladding:

$$A = \frac{\sqrt{3}Pitch^2}{4} - \frac{3R_{clad\ ext}^2}{360} 60 = 2.42 \cdot 10^{-5} \text{ m} \quad (6.21)$$

Heated perimeter of single tube is 0.022 m and the hydraulic diameter (D_{hyd}) is calculated like ratio of area of mass flow and perimeter of heat transfer surface multiplied by 4 and it is equal to 0.0045 m.

Mass balance coolant:

$$\sum_{i=1}^{N-1} \frac{dM[i]}{dt} = \frac{w_{in} + w_{out}}{N_t} \quad (6.22)$$

Momentum balance of coolant:

$$\frac{L}{A} \cdot \frac{dw}{dt} = (p_{out} - p_{in}) + \Delta p_{st.head} + \Delta p_{friction} \quad (6.23)$$

Energy balance of coolant:

$$A \cdot l \cdot \rho[i] \cdot \frac{dh[i]}{dt} + w[i] \cdot (h[i + 1] - h[i]) = Q_{single}[i] \quad (6.24)$$

Where $\frac{dM[i]}{dt}$ is the time derivative of mass in each cell between two nodes; Q_{single} - heat added to the coolant in segment i (W); w - mass flow rate (kg/s).

In the simulation of the primary side, it is assumed that static head and friction pressure drops play a significant role. These pressure drops are calculated according to Idelchik [18]. Value G in equation for frictional pressure drop refers to mass flux ($kg/m^2/s$), calculated as the product of velocity of the moderator inside the core and its average density. The fanning friction factor (f) has been appropriately set in the circulation loop to comply with the estimated mass flow rate. Coefficients A and m are taken for turbulent flow, with the values of 0.079 and 0.25, respectively:

$$\Delta p_{friction} = \frac{fG^2 \frac{1}{\rho} L}{2 \cdot \emptyset} \quad (6.25)$$

$$\Delta p_{st.head} = \rho g L \quad (6.26)$$

$$f = \frac{A}{Re^m} \quad (6.27)$$

Therefore, the nominal value for friction pressure drop of moderator in the reactor core is 20 kPa, assuming that fanning factor is 0,0037.

Distributed heat transfer model with constant coefficient is assumed at the interface with the fluid. The heat transfer coefficient depends on the coolant mass flow rate condition

as well as on core geometry and it can be estimated using the Dittus-Boelter correlation, valid for turbulent flow in narrow channels.

$$Nu = 0.023 \cdot Re^{0.8} Pr^{0.4} \quad (6.28)$$

$$h = \frac{Nu \cdot k}{L} \quad (6.29)$$

6.1.4 Other components of primary circuits

The mass flow of coolant from the reactor core to the steam generator is described by the Riser component. This single tube has a length of 2.3 meters and a diameter of 0.65 meters. The total mass flow rate of the coolant is 902.8 kg/s. The proper functionality of this component is ensured by the implementation of mass balance, momentum balance, energy balance, and frictional pressure drop.

The Downcomer component, located after the steam generator, performs the same functions as the Riser, using the same set of equations and geometric properties, but has a length of 1.5 meters.

Due to the lack of detailed geometrical and physical information about the gaseous pressurizer for the RITM-200, a simple pressure sink was used instead. It functions similarly to a pressurizer by regulating pressure.

The “ThroughMassFlow” component was used in place of a pump to simplify the model. This component prescribes the flow rate passing through it during forced convection and includes basic equations for mass balance and energy balance.

6.2 Steam generator

The primary circuit is coupled with the secondary side through four steam generators to transmit 175 MW of thermal power. Each of these heat exchangers has been modeled as a cassette-type straight-tube steam generator, using Finite Volume Models (FVM) for 1-dimensional distributed-parameter modeling of water/steam flow interfaced with a metallic wall component. Each 1-D tube flow model represents either the primary or secondary side of the heat exchanger. The component “CounterCurrentFV” located between the primary side and the metal tube defines the model for counter-current heat transfer (see Fig. 18).

Two hydraulic circuits are connected to the steam generator through 2 inlet and 2 outlet ports: the forced circulation loop in the primary circuit pushes water from the top of the steam generator to the bottom of the core. The elevation of the outlet over the inlet is 1.9 meters. Each heat exchange tube has diameters of 8 mm and 13 mm for the primary and secondary fluids, respectively.

In the modeling of this component, the number of tubes has been assumed equal to the original number taken from literature. One steam generator consists of 3 cassettes, every single cassette has 7 moduli with 118 tubes in each modulus. Therefore, total amount of tubes in one SG is 2478. The total thermal exchange area according to available data is 280 m².

From a computational standpoint, using such an advanced geometry can require substantial computational power. Therefore, the pseudo-regenerative region of the heat

exchanger (Fig. 13, a), where feed water interacts with steam, was excluded from the modeling (Fig. 19). Consequently, the length of the tubes in the steam generator (SG) decreases from 2 meters to 1.9 meters. This reduction leads to a decrease in the total heat transfer area by 14 m^2 , resulting in a new total of 266 m^2 .

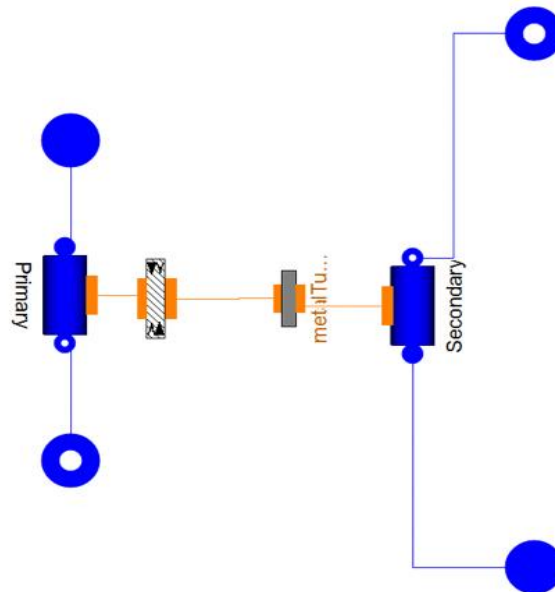


Figure 17: Model of steam generator

The removal of the pseudo-regenerative region eliminates the intermediate point where steam reaches 303°C (Fig. 13, b). Moreover, according to [8], the inlet temperature of feed water for the land-based RITM-200 is not the same as that for the marine-based version (105°C), but is instead 170°C .

Based on the information above, the SG exhibits a straightforward increase in feed water temperature from 170°C to 295°C . The range of coolant temperature passing through the SG remains similar to that in the icebreaker, decreasing from 313°C to 277°C .

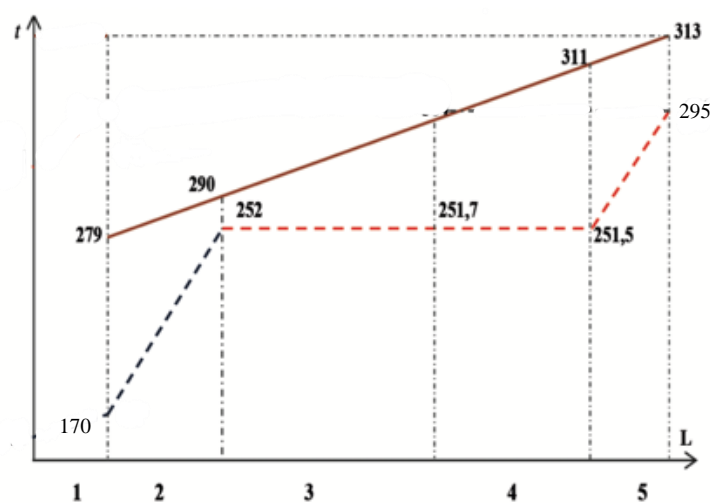


Figure 18: Temperature distribution of primary and secondary fluids without pseudo-regenerative region.

The metal walls component is equivalent to the overall surface of the tube bundle between the primary and secondary side of the mass flow, with titanium alloy properties. A constant heat transfer coefficient ($h_{secondary}$) has been assumed for the secondary side of the heat transfer model, due to phase transition of secondary side's fluid. It was calculated through the formula represented below and equal to $1,66 \cdot 10^4 \frac{W}{m^2K}$. For the primary side Dittus-Boelter correlations was selected to compute heat transfer coefficient of the coolant ($h_{primary} = 2,32 \cdot 10^4 \frac{W}{m^2K}$).

$$h_{secondary} = \frac{q'}{2 \cdot \pi(T_{wall} - T_{sat})R_{ext}} \quad (6.30)$$

Where q' is linear heat rate for two phase mixture, T_{wall} – average temperature of tube, T_{sat} – saturation temperature of water for 34 bars, R_{ext} is external radius of tube of steam generator.

Primary side flow and secondary side flow components work in the same way as for the reactor core model using the same set of equations describing momentum balance, mass balance, energy balance and pressure drop calculations.

“CounterCurrentFV” component allows the temperature and flux vectors on one side to swap with respect to the other side. This means that the temperature of node j on side 1 is equal to the temperature of note $N-j+1$ on side 2.

“MetalTubeFV” component describes behavior of cylindrical tube made of titanium alloy PT-7M with thermal conductivity (λ) equal to $12 \frac{W}{m \cdot K}$ and the heat capacity per unit volume is defined by multiplication of specific heat capacity and density of the alloy and it is equal to $2806.25 \frac{J}{m^3 \cdot K}$. Resistance of the wall is calculated based on Fourier equation:

$$Wall\ resistance = \frac{\ln \frac{R_{ext}}{R_{int}}}{2 \cdot \pi \cdot \lambda} \quad (6.31)$$

6.3 Secondary side model

As depicted in Figure 20, the heat engine system employs a closed Rankine cycle to achieve heat-work conversion, providing a highly efficient method of generating power. The system comprises several key components, including a turbine, condenser, recuperators, deaerator, and pipes. These components work together to ensure the efficient transfer of thermal energy from the primary fluid to the working medium. The modeling of the turbine was carried out using the ThermoPower library.

In the available literature, it was challenging to find detailed information about pressure and enthalpies after each stage of the turbine. Therefore, it was decided to use the EBSILON professional application, where the parameters of steam at the outlet and inlet of the steam generator (SG) are fixed, when steam cycle was optimized in terms of operational points (pressure, enthalpy) to maximize the electrical power output and to determine all quantities of steam in each part of the turbine and the secondary side in

general (see Fig. 20). You can see that the optimization result of gross power of 56.7 MWe is consistent with literature [7] value of net power of 55 MWe.

Consequently, information received from application is used like reference data for dynamic simulation of balance of plant for RITM-200.

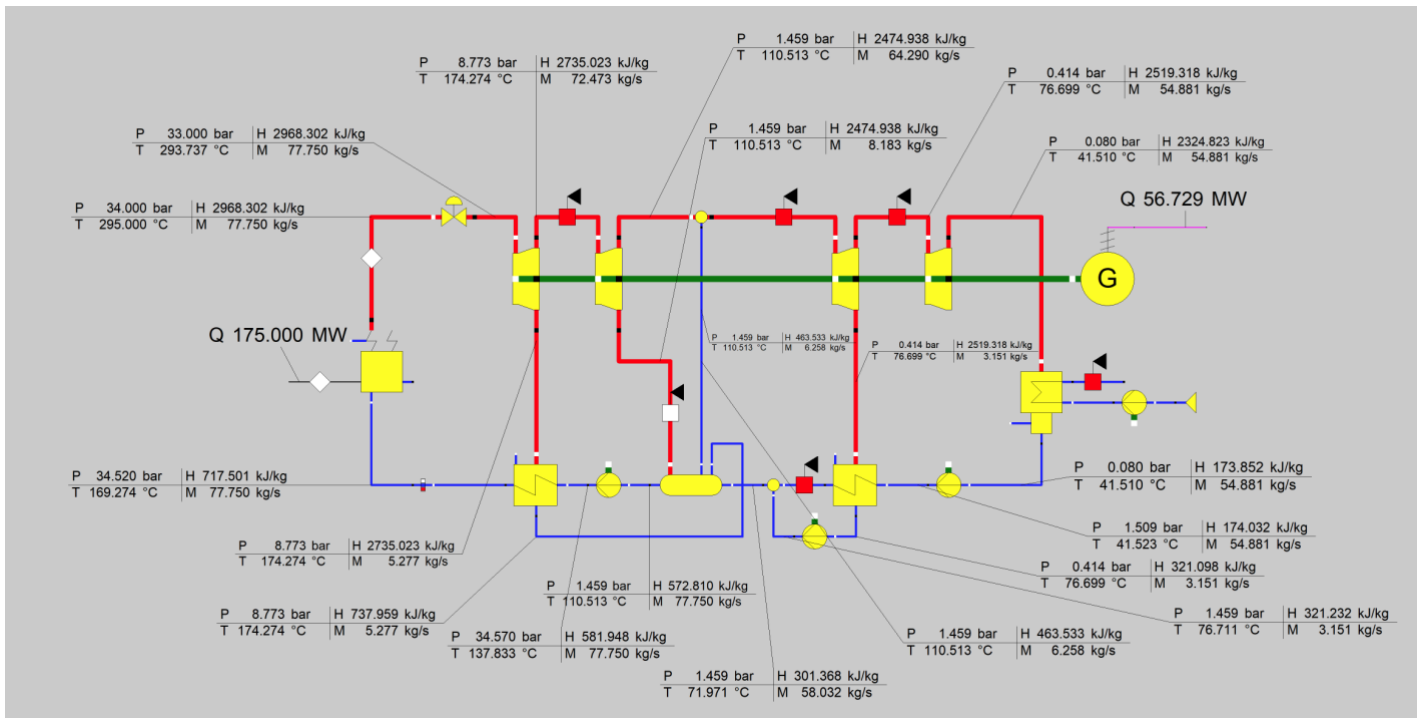


Figure 19: Model of secondary circuit made in EBSILON professional

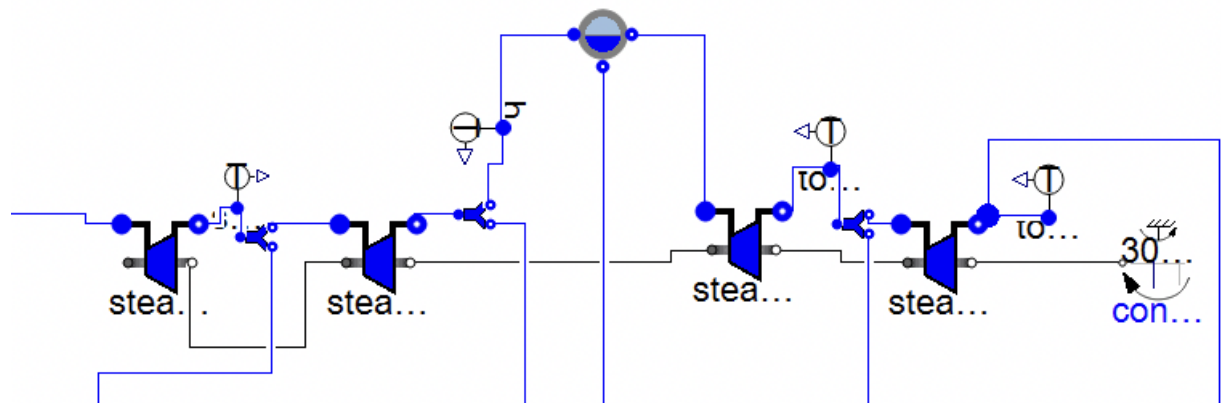


Figure 20: Model of steam turbine with separator.

The steam enters the turbine (Fig. 21), where it expands and performs work driving the main shaft to rotate. The nominal rotation speed of the rotor is 3000 rpm. Performed model produces 55 MW of electric power.

Between two sections of turbine there is a steam separator, it is important in order to remove water drops from steam to improve quality of steam and protect the turbine. High pressure section of turbine provides steam for regenerative heater and deaerator, low pressure section has one branch for regenerative heater.

This is implemented by extracting or bleeding small quantities of steam from suitable points throughout the turbine stages, utilizing the heat content of the extracted or bled

steam. The vessels where the exchange of heat takes place are called regenerative heaters. Here, the steam totally condenses, and the outlet water leaves the heater with a higher temperature. The main advantage of regenerative feed water heating is the reduction of steam consumption in the condenser and losses in it. The turbine condensate, which receives the heat of the spent steam, serves as a cold source for regenerative selection steam. Accordingly, the heat consumption for steam generation in the steam generator decreases, and cycle efficiency increases.

Superheated steam with temperature $T = 295^{\circ}\text{C}$ and pressure $P = 34$ bar passes through steam turbine K-50-3,4/50 with two regenerative heaters. Every stage of the turbine is modelled considering Stodola's law. This law is important for the relation between pressure and mass flow. It states that the maximum theoretical efficiency of a steam turbine depends on the temperature drop between the steam entering and leaving the turbine:

$$\dot{m} = -K_t \sqrt{\rho p_{in}} \sqrt{1 - \frac{p_{out}^2}{p_{in}^2}} \quad (6.32)$$

Where K_t is the coefficient linking pressure and mass flow. Since K_t is the only one unknown value, this equation is used to calculate Stodola's coefficient for each turbine stage. Calculated data are listed in Table 12.

Table 12: Stodola's coefficient and pressures of each stage of turbine.

| Stage of turbine | Stodola's coefficient, K_t | Inlet pressure, MPa | Inlet temperature, $^{\circ}\text{C}$ | Outlet pressure, MPa | Outlet temperature, $^{\circ}\text{C}$ |
|------------------|------------------------------|---------------------|---------------------------------------|----------------------|--|
| Stage 1 | 0.0117 | 3.3 | 295 | 0.863 | 174 |
| Stage 2 | 0.0375 | 0.877 | 174 | 0.146 | 110 |
| Stage 3 | 0.151 | 0.146 | 110 | 0.0414 | 76.7 |
| Stage 4 | 0.477 | 0.0414 | 76.7 | 0.008 | 41.5 |

According to the reference data it was assumed that mechanical efficiency (η_{mech}) of a turbine's stage is 1 and isentropic efficiency (η_{iso}) is 0,85. Consequently, several equations describing outlet enthalpy, mechanical power from the steam, mechanical power balance and mass balance were introduced to model the steam turbine:

$$h_{in} - h_{out} = \eta_{iso}(h_{in} - h_{iso}) \quad (6.33)$$

$$P_m = \eta_{mech} \dot{m}(h_{in} - h_{out}) \quad (6.34)$$

$$P_m = -\tau\omega \quad (6.35)$$

$$\dot{m}_{in} + \dot{m}_{out} = 0 \quad (6.36)$$

Where P_m is mechanical power, h_{iso} - isentropic outlet enthalpy, τ is the net torque acting on the turbine, ω - shaft angular velocity.

There, between high- and low-pressure sections of turbine, is located separator without intermediate heater. Steam separation before the last stages of the turbine is important in order to avoid a significant decrease in the internal efficiency of the turbine and unacceptable erosion of the turbine blades. Saturated steam passing through the separator experiences decrease of temperature by 1°C and almost negligible reduction of pressure. Condensed steam goes back to the feed water zone of secondary circuit through deaerator.

After the turbine steam with temperature equal to $41,4^{\circ}\text{C}$ passes through the condenser. The pressure of condensed water is 8 kPa. For the modeling of this condenser energy and mass balance equations were used:

$$\frac{dM}{dt} = \dot{m}_{in} + \dot{m}_{out} \quad (6.37)$$

$$\frac{dE}{dt} = \dot{m}_{in} h_v + \dot{m}_{out} h_l - Q \quad (6.38)$$

Then pump, which is a "ThroughMassFlow" component in this case, increases pressure from one atmosphere to 1,5 atmospheres. It is equal to the pressure level inside the deaerator.

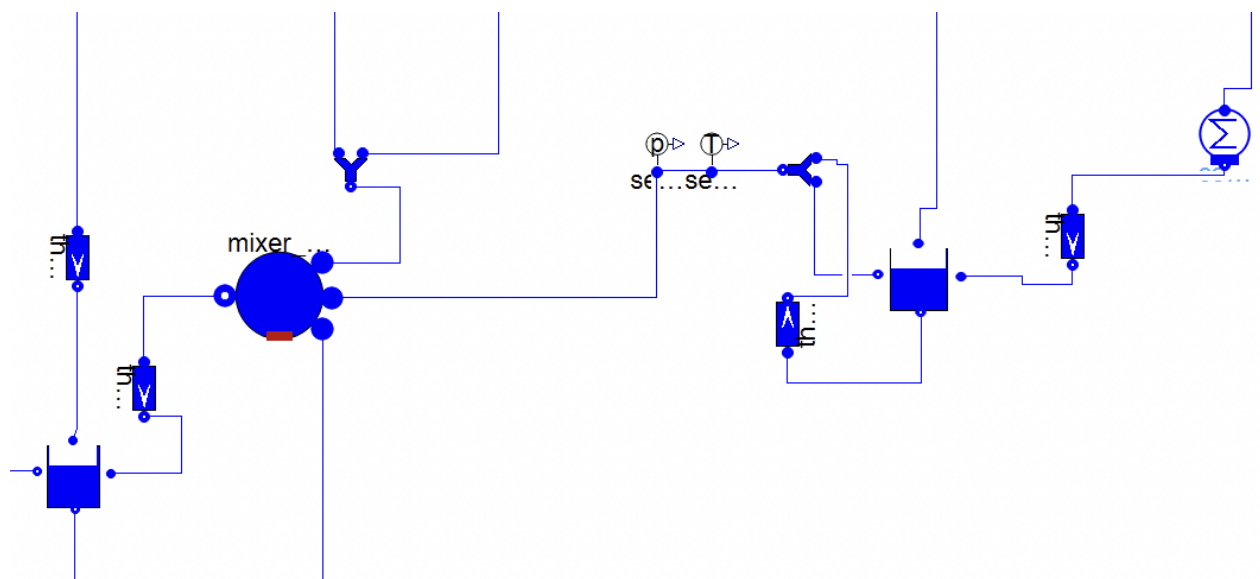


Figure 21: Model of feed water part of secondary circuit.

After the pump feed water goes to regenerative counter-flow heat exchanger, where steam coming from low pressure section of turbine transmit heat to the feed water (Fig. 22). For simplification purpose, the heat exchanger was modelled like zero-dimensional one, therefore geometric dependance is looped in the global conductance. It contains equations of mass and energy balances of stem and feed water and heat transfer equation:

$$Q = K \cdot \Delta T \quad (6.39)$$

$$\Delta T = \frac{\Delta T_A - \Delta T_B}{\ln \frac{\Delta T_A}{\Delta T_B}} \quad (6.40)$$

Where Q is the thermal power, K – global heat transfer coefficient calculated like a multiplication of heat transfer coefficient and area of heat flow, ΔT – is the logarithmic mean temperature difference, which is used to determine the temperature driving force for heat transfer in heat exchangers.

Moreover, due to the lack of information about the material of the tubes in the heat exchanger, it was decided not to use the metal tube component. Therefore, inertia of the wall and of the fluid mass are neglected. After the thermal interaction with steam, the temperature of the feed water increases from 41.4°C to 72°C. The outlet of the condensed steam is connected to the feed water pipeline.

Next component of the secondary circuit side is the deaerator. The main function of this tool is to remove dissolved gases from feedwater. This component's model is based on a water tank model. It has four inlets and one outlet (Fig. 27). Feed water coming to the deaerator's volume is heated by steam entering from the high-pressure section of the turbine separator ($T=110,5^\circ\text{C}$ in both pipes) and condensed steam ($T=172^\circ\text{C}$) flowing from the last regenerative heater. On the outlet of the deaerator, feed water reaches a temperature equal to 110°C.

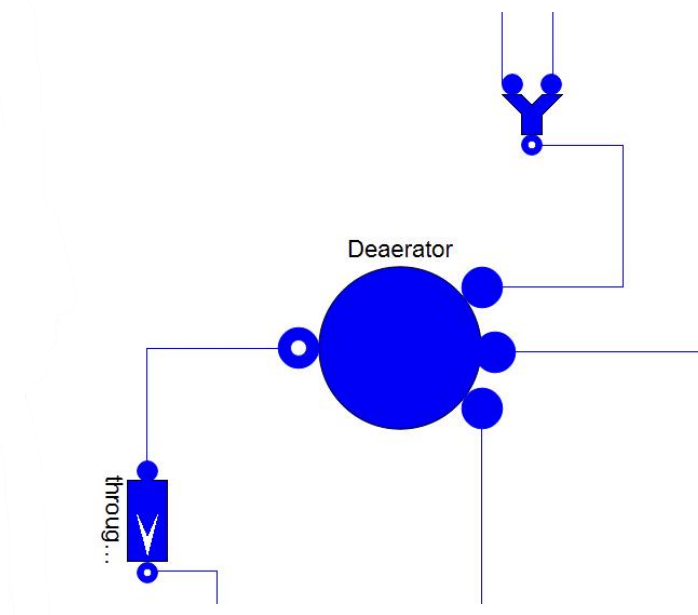


Figure 22: Model of deaerator.

The functionality of the deaerator model is provided by fluid mass and energy balances, similar to the equations used for the component describing the compressor.

The following pump increases the pressure of the secondary side up to 3.4 MPa and pushes feed water to the second zero-dimensional regenerative heat exchanger, where steam with a temperature of 174°C comes from the high-pressure section of the turbine.

The condensed steam then returns to the deaerator. Simultaneously, the feed water reaches 170°C and proceeds to the bottom part of the steam generator.

6.4 Passive residual heat removal model

The Passive Residual Heat Removal System (PRHRS) is crucial for the safety of a nuclear power plant. It functions during emergencies, such as a loss of coolant flow, enabling the reactor to transfer decay heat without requiring human, electrical, or mechanical intervention. This significantly enhances the inherent safety of the NPP. Typically, the PRHRS is designed to operate passively for up to 3 days [8].

The PRRS activates in the event of a blackout when active systems are unavailable. At this time, the control rods are fully inserted into the reactor core, absorbing neutrons and halting power production. However, this does not mean that thermal power drops to zero; fission products continue to undergo radioactive decay according to the decay law (Fig. 24). The initial thermal power from this decay is 6% of the nominal value, which for the RITM-200 is approximately 10.5 MW. The decay power changes over time according to the following law [8]:

$$Q_{residual} = 6 \cdot 10^{-2} \cdot Q_{nominal} (\tau^{-0,2} + (\tau + T)^{-0,2}) \quad (6.41)$$

Where τ is an operational time of PRHRS, T is a time of operation at nominal power until complete insertion of control rods. Operation time at nominal power is much larger than duration of shutdown therefore variable $(\tau + T)^{-0,2}$ tends to zero.

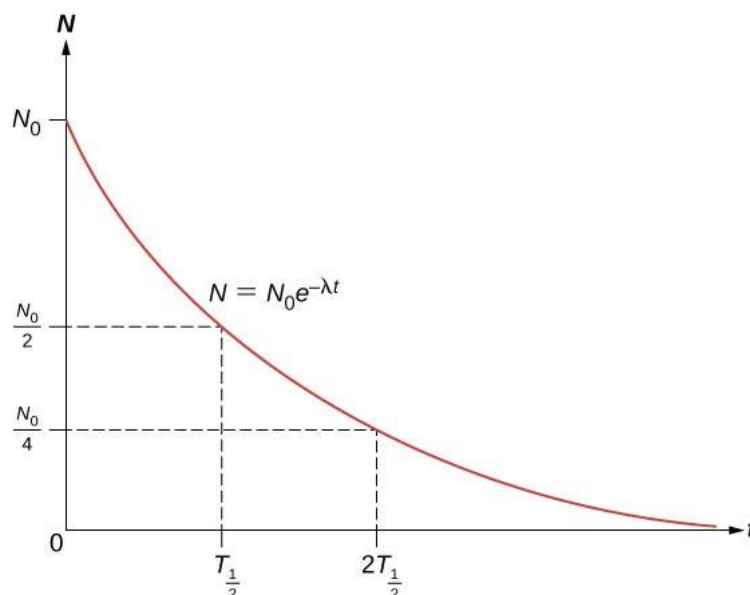


Figure 23: Radioactive decay law

The PRHRS consists of two steam generators with a geometry similar to those used during normal operation, two air heat exchangers (AHX) functioning as air towers, and two water heat exchangers (HX) containing boiling water tanks that interact with atmospheric air. The heat removal process is facilitated by natural circulation, driven by the hydrostatic pressure difference between the top and bottom of the heat exchanger, which generates a buoyancy force. When this buoyancy force equals the pressure drop in the virtual natural circulation loop, a steady-state mass flow rate is established in the circuit. The Dymola solver calculates the state system balance equations associated with the model and determines the solution for the natural circulation mass flow rate.

The model of the PRHRS is illustrated in Figure 25. It consists of three circuits: the first removes residual heat from the reactor core, the second is an open loop connected to the air heat exchanger, and the third is a closed loop with boiling water in a water tank.

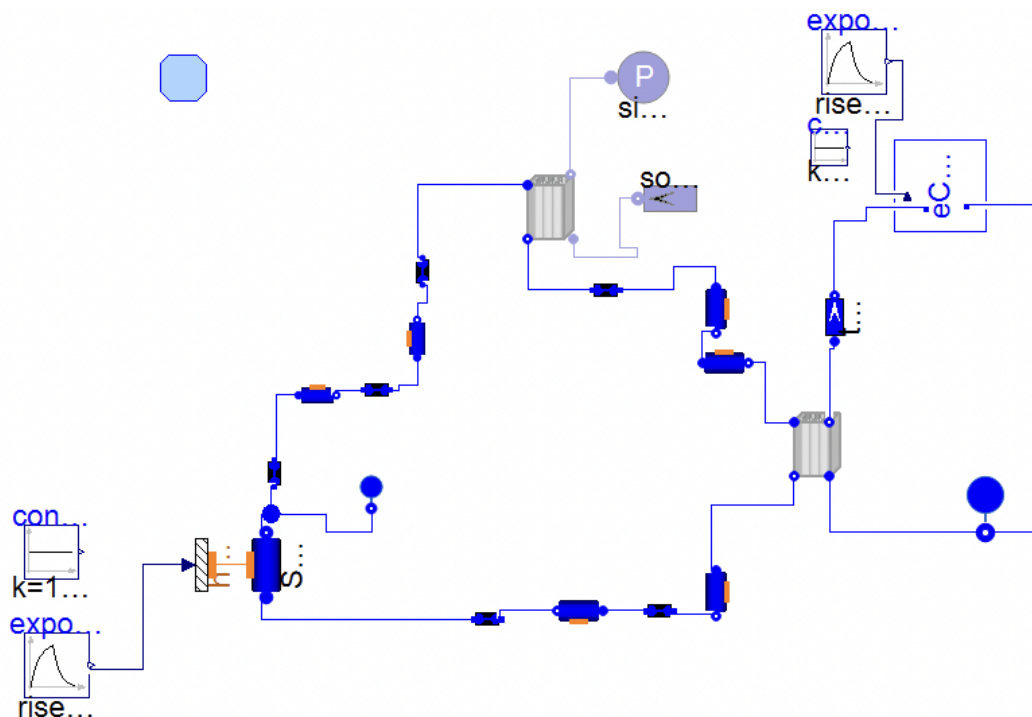


Figure 24: Passive residual heat removal model.

Due to the limited data available on the geometry and properties of such safety systems, several assumptions were made. The geometry of the main heat exchanger is based on the characteristics of the steam generator, with the same number of tubes and total length. Subcooled water, with a mass flow rate of 5 kg/s calculated through energy balance, enters the steam generator at 90°C and 2 MPa. After the phase transition, it exits as saturated steam at 200°C. The reactor's primary side is not modeled; instead, the secondary side of the heat exchanger is directly connected to an ideal heat exchanger functioning as a thermal source, which describes decay power generation.

The steam generator is designed as a tube-inside-tube configuration. The internal radius of the tube for coolant is 4 mm, with a tube thickness of 1.5 mm, and the outer radius for the working fluid is 6.5 mm. After leaving the steam generator, the saturated steam flows to the air heat exchanger, which acts as an air tower where atmospheric air at ambient temperature removes 30% of the total residual heat, initially equal to 3.15 MW.

Consequently, the saturated steam condenses into saturated water. Given the lack of specific information, it was assumed that the tube material for the heat exchangers is the same titanium alloy used in the steam generator tubes.

The PRHRS model depicted in Figure 25 encounters an issue related to the additional circuit connecting the water HX and ECD tank. Specifically, a "ThroughMassFlow" component is included to simulate the function of a pump, ensuring the prescribed flow rate through this circuit. Without this component, simulating natural circulation in this part of the system becomes problematic and ineffective. Thus, the "ThroughMassFlow" component is crucial for maintaining the intended operation of the PRHRS model in this context.

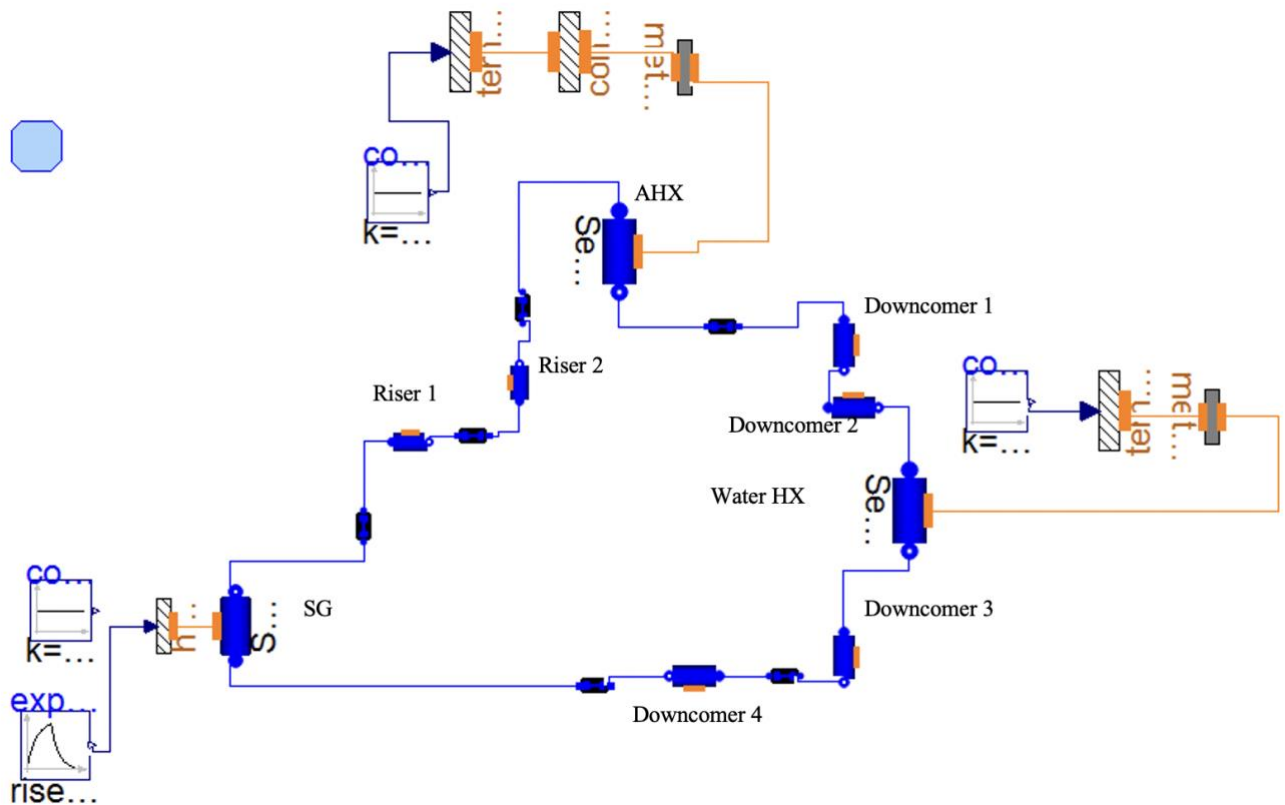


Figure 26: Model of PRHRS with temperature boundary conditions

To address the issues encountered with the previous PRHRS model, a new approach has been implemented as depicted in Figure 26. The primary difference in the new model is the replacement of the AHX, water-water HX, and ECD tank loop with temperature sources serving as boundary conditions for the system. This change was motivated by several considerations.

Firstly, the forced circulation within the additional loop posed challenges, leading to its exclusion from the model to focus on the core passive circuit. Secondly, there was a shift in the calculation logic. In the new model, constant temperature sources of 35 °C and 100 °C were introduced, mimicking the role of AHX and water-water HX respectively. These temperatures were chosen based on typical atmospheric conditions. Additionally, a cylindrical tube component was incorporated to manage thermal resistance, replacing real air and water in the AHX and water-water HX.

Under this revised approach with boundary conditions, the PRHRS model now calculates the distribution of absorbed power between the HXs autonomously. In contrast to the previous model where specific power removal percentages were initially defined (30% by AHX and 70% by water-water HX), the new model dynamically determines the thermal distribution.

This approach ensures improved simulation accuracy and flexibility, aligning the model closely with operational conditions and enhancing the overall performance assessment of the PRHRS.

Steam generator, AHX and water-water heat exchangers experience phase transition inside the tubes. Due to this phenomena, calculation of heat transfer coefficient is a serious challenge. It was decided to use Shah correlation which works for accurate prediction of heat transfer during condensation and evaporation [19]. It was verified with data for mini and macro channels from 130 sources for 51 fluids covering an extreme range of parameters. In this case HTC for the mixture is calculated like a summation of two convective coefficients:

$$h_{TP} = h_I + h_{Nu} \quad (6.42)$$

$$h_{Nu} = 1.32 \cdot Re_{LS}^{-\frac{1}{3}} \left[\frac{\rho_L (\rho_L - \rho_G) g k_L^3}{\mu_L^2} \right]^{\frac{1}{3}} \quad (6.43)$$

$$h_I = h_{LS} \left(1 + \frac{3.8}{Z^{0.95}} \right) \left(\frac{\mu_L}{14\mu_G} \right)^{(0.0058+0.557p_r)} \quad (6.44)$$

$$h_{LS} = 0.023 \cdot \frac{Re^{0.8} Pr^{0.4} k_L}{D} \quad (6.45)$$

$$p_r = \frac{P}{P_{reduced}} \quad (6.46)$$

$$Z = \left(\frac{1}{x} - 1 \right)^{0.8} \cdot p_r^{0.4} \quad (6.47)$$

Where Z – Shah's correlating parameter, h_I – HTC for stratified law, h_{LS} - heat transfer coefficient assuming liquid phase flowing alone in the tube, p_r – reduced pressure

Based on these equations heat transfer coefficients of two-phase mixture were calculated for each heat exchangers:

$$HTC_{SG} = 18990 \text{ W/m}^2\text{K}; HTC_{AHX} = 6,07 \cdot 10^3 \text{ W/m}^2\text{K}; HTC_{ECD} = 8,9 \cdot 10^3 \text{ W/m}^2\text{K}$$

The final step of the thermal analysis of the heat exchangers involves calculating the total heat exchange area (A) to determine the total number of tubes required. This calculation can be done using the overall heat transfer coefficient [W/K] and the heat transfer equation. Length of AHX tubes is 2 meters, length of water HX's is 1,5 meters. The total number of tubes in the air heat exchanger (AHX) is 1149, while for the water heat exchanger (HX), this value is 231. h_{int} and h_{ext} for water HX are calculated using Shah correlation. As for AHX, h_{ext} is taken from Dittus-Boelter correlation.

$$U = \frac{1}{\frac{1}{h_{int}} + \frac{r_{ext}}{k} \ln \frac{r_{ext}}{r_{int}} + \frac{1}{h_{ext}}} \quad (6.48)$$

$$A = \frac{Q}{U\Delta T} \quad (6.49)$$

$$N_t = \frac{A}{3,14 \cdot \phi \cdot L} \quad (6.50)$$

Given the passive nature of the system, it must function reliably without electricity, necessitating stringent inherent safety requirements. As such, the system does not utilize any pumps; instead, the flow of the two-phase mixture is driven entirely by natural circulation. Therefore, accurately calculating all pressure drops within the model is crucial to ensure its effective operation and reliability.

Using correlations provided by Idelchik's reference book [18] gravitational, frictional, and local pressure drops were calculated. General formulas are presented below. Pressure losses along the length of a straight pipe of constant cross-section are calculated using the Darcy-Weisbach formula:

$$\Delta p_{friction} = \lambda \frac{l}{D_{hydr}} \cdot \frac{\rho w_0^2}{2} \quad (6.51)$$

Formula for coefficient of friction resistance depends on type of flow. The type of flow is determined of Reynolds number. Low value of Reynolds number (<2000) leads to laminar flow, turbulent flow happens when $Re > 4000$. In PRHRS model flow is turbulent in every section of tubes, therefore, friction resistance is calculated using following correlation:

$$\lambda = \frac{l}{(2lg \frac{3,7}{\bar{\Delta}})^2} \quad (6.52)$$

$\bar{\Delta}$ is the roughness of inner surface of tubes, this value is equal to $0.6 \mu m$ for titanium alloy tubes [20].

Gravitational pressure drop in a piping system is caused by fluid rising in elevation and assessed according to:

$$\Delta p_{gravitational} = \rho g l \quad (6.53)$$

All these values were calculated for each heat exchanger, riser and downflow of the model and represented in Table 13.

Table 13: Gravitational and frictional pressure drop of PRHRS (Fig. 26)

| Component | Pressure drops, kPa |
|-----------------|---------------------|
| Steam generator | |
| - Frictional | 1,6 |
| - Gravitational | 8,1 |

| | |
|-----------------|--------|
| Riser 1 | |
| - Frictional | 19,343 |
| - Gravitational | 0,848 |
| Riser 2 | |
| - Frictional | 21,278 |
| - Gravitational | - |
| AHX | |
| - Frictional | 0,138 |
| - Gravitational | 3,516 |
| Downcomer 1 | |
| - Frictional | 0,228 |
| - Gravitational | 1,720 |
| Downcomer 2 | |
| - Frictional | 0,023 |
| - Gravitational | - |
| Water-water HX | |
| - Frictional | 2,062 |
| - Gravitational | 8,943 |
| Downcomer 3 | |
| - Frictional | 0,186 |
| - Gravitational | 59,4 |
| Downcomer 4 | |
| - Frictional | 0,26 |
| - Gravitational | - |

Speaking about local pressure drops there were considered 90-degree rotation in the pipes. Looking at figure 7, it is obvious that system has seven local pressure drops. Three bends on the way from steam generator to air heat exchanger, two bends from air heat exchanger to water-water heat exchanger and two bends from water-water heat exchanger to steam generator. All formulas are taken from Idelchik's reference book. [18]

The coefficient of local resistance of taps is calculated according to the formula proposed by Abramovych:

$$\zeta_M = \frac{\Delta p}{\frac{\rho w_0^2}{2}} = A_1 B_1 C_1 \quad (6.54)$$

Where A_1 is a coefficient that takes into account the influence of the angle δ of the curvature of the tap. B_1 is a coefficient that considers the influence of the relative radius $R_0/D_0(R_0/b_0)$ of the curvature of the tap. C_1 is a coefficient that considers the influence of the relative elongation of the cross section from water a_0/b_0 .

The value of A_1 is found according to Nekrasov [18]: if angle $\delta = 90^\circ$, then $A_1 = 1$. The value of B_1 can be calculated from graphs b and c of Diagram 6-1, and the value of C_1 can be calculated from graph d of diagram 6-1. Therefore, for 90-degree rotation in the pipes: $A_1 = 1, B_1 = 0,21, C_1 = 1$.

Consequently, local pressure drop depends on relation below which values are represented in the Table 14.

$$\Delta p = \frac{\zeta_M \rho w_0^2}{2} \quad (6.55)$$

Table 14: Local pressure drops of PRHRS

| Number of the pipe's tap | Value of pressure drop, kPa |
|--------------------------|-----------------------------|
| 1 | 5,96 |
| 2 | 5,96 |
| 3 | 5,96 |
| 4 | 5,96 |
| 5 | 0,134 |
| 6 | 0,134 |
| 7 | 0,54 |
| 8 | 0,54 |

7 Results of modelling

7.1 Steady state simulation of primary and secondary circuits

The objective of the first experiment was to evaluate the performance of the coupled primary and secondary circuits of the SMR RITM-200 (Fig. 15) during steady-state simulation. The aim was to verify that the modeled system produces results comparable to reference data. The reactor was brought to its nominal power and maintained at 175 MW throughout the simulation. During this period, the cooling system transferred thermal power to the secondary circuit, leading to electricity generation.

Figure 28 illustrates the thermal power generated in the core, the inlet and outlet temperatures of the coolant and feed water from the steam generator (SG), the steam quality inside the SG, and the total electrical power generated by the turbine.

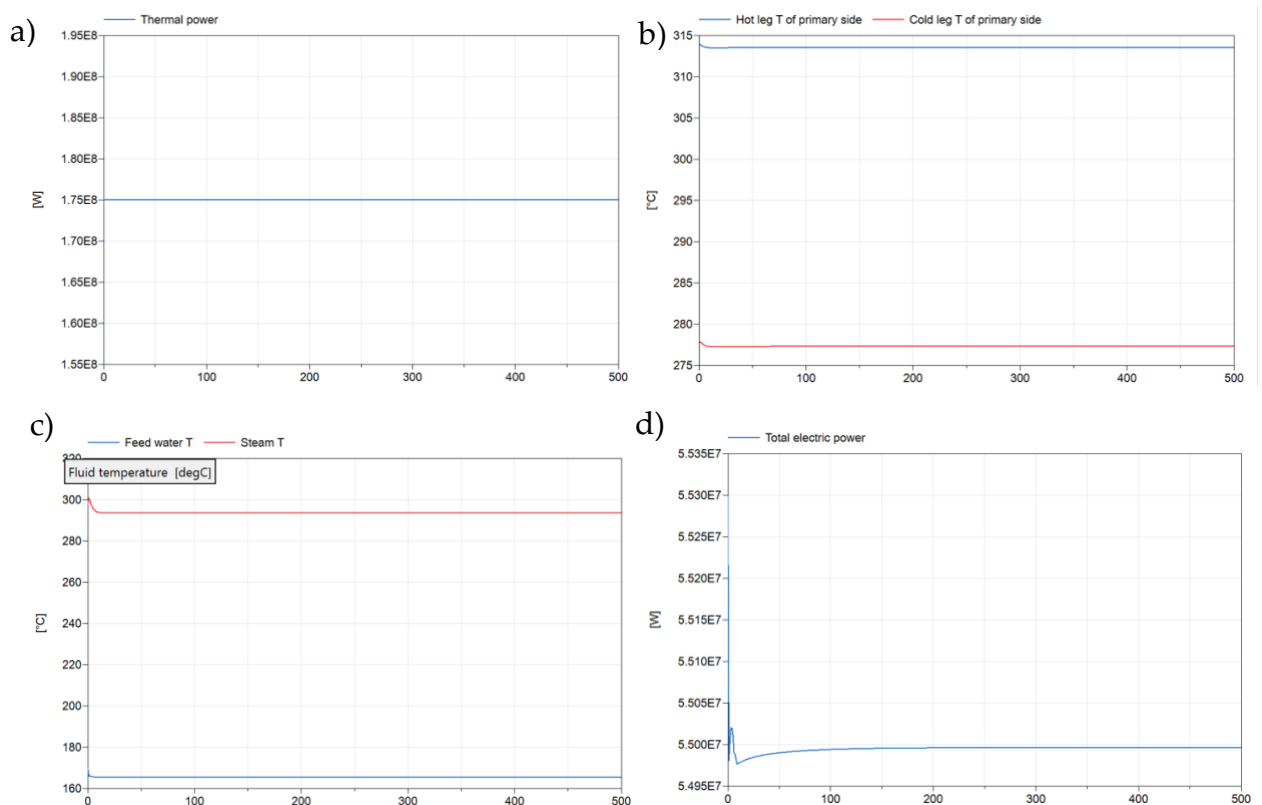


Figure 25: Results of steady state simulation of primary and secondary sides.

a – Thermal power, b – Inlet and outlet temperatures for primary side, c – Inlet and outlet temperatures for secondary side, d – Total electric power

As observed, the modeling results align closely with the reference data (Table 15). The thermal power is 175.2 MW, with the coolant temperature varying from 277.3°C to 313°C. On the secondary side, the temperature increases from subcooled conditions ($x=0$) to superheated steam ($x=1$). Similarly, the steam turbine generates 55 MW of electric power.

Table 15: Comparison of reference and modelled data

| Quantity | Modelled values | Reference data |
|--|-----------------|----------------|
| Thermal power, MW | 175,2 | 175 |
| Electric power, MW | 55 | 55 |
| Mass flow rate of primary side, kg/s | 902,8 | 902,8 |
| Mass flow rate of secondary side, kg/s | 77,75 | 72.5 |
| Inlet temperature of coolant, °C | 313,5 | 313 |
| Outlet temperature of coolant, °C | 277,5 | 277 |
| Inlet temperature of feedwater, °C | 165,9 | 170 |
| Outlet temperature of steam, °C | 294,1 | 295 |
| Pressure of primary side, MPa | 15,7 | 15,7 |
| Pressure of secondary side, MPa | 3,4 | 3,4 |

Some figures display noticeable but not dramatic fluctuations at the beginning of the simulation. It is suggested that these occur because Modelica searches for appropriate steady-state conditions, which affects the initial values.

7.2 Load following simulation

Second experiment is the simulation of load-following process. Load following in a nuclear reactor refers to the ability of the reactor to adjust its power output to match changes in demand for electricity on the electrical grid it is connected to. This capability is important because the demand for electricity fluctuates throughout the day due to factors such as changes in weather, economic activity, and human behavior.

Here are some key strategies used for load following in LWRs [21]:

1. Sliding Pressure Control

Sliding pressure control is a method where the pressure of the steam generator or reactor coolant system is varied to control the reactor power output. The basic principle involves changing the reactor's thermal output by adjusting the pressure setpoint of the steam generators.

2. Reactor Power Level Control

This strategy involves directly adjusting the reactor's power output through control rods or boron concentration (for pressurized water reactors, PWRs).

3. Turbine Control

Turbine control involves adjusting the turbine governor to change the steam flow to the turbine, thereby controlling the electrical output.

Figure 29 illustrates the arrangement of components for the load-following analysis using the turbine control approach. This model features an open-circuit arrangement on the secondary side. This simplification was made to streamline the modeling process, as the primary value influenced by the control system is the electric power output of the steam turbine. Consequently, the other components of the secondary side hold less importance for this specific analysis.

The key regulation component is the PI controller. A PI controller, short for Proportional-Integral controller, is a type of feedback control system widely used in various industries and applications to regulate processes and systems. It combines two control actions. The proportional action provides a control output that is directly proportional to the current error signal, which is the difference between the desired setpoint and the actual process variable. The proportional term contributes to reducing the steady-state error and provides an immediate response to changes in the error. Integral action integrates the error signal over time and generates a control output proportional to the accumulated past errors. It helps eliminate steady-state error by continuously adjusting the control output until the error converges to zero. The integral term addresses any systematic bias or offset in the system. [22]

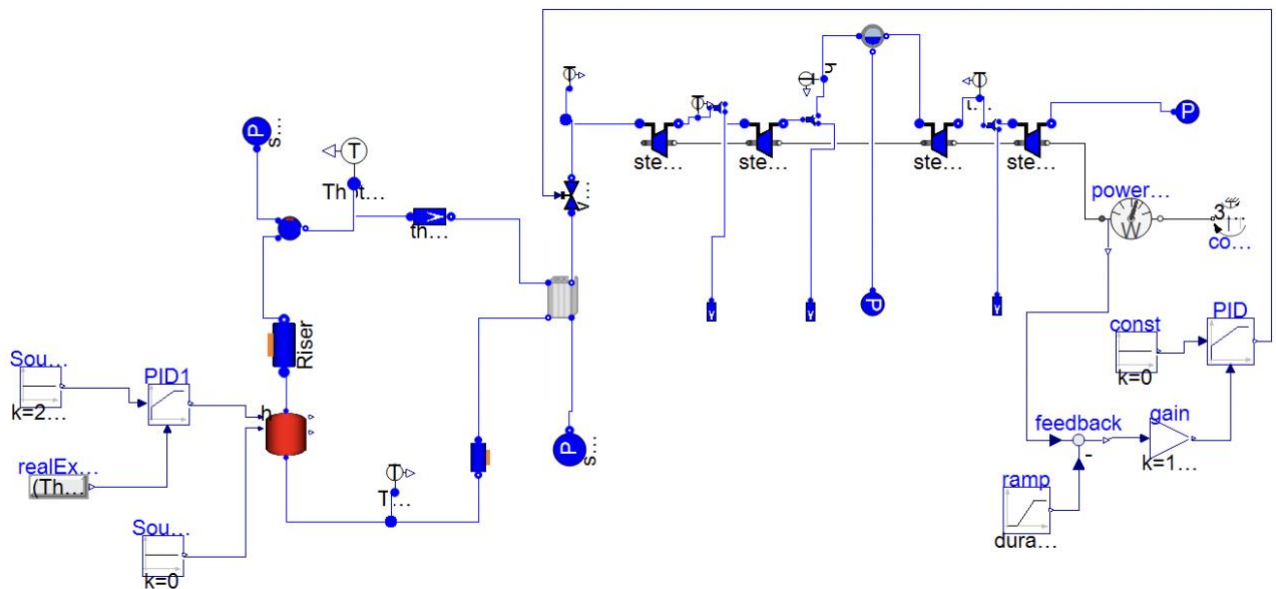


Figure 26: Model of load following simulation

This model has two PI controllers for primary and secondary sides.

The PI controller of the secondary side has two inputs. The first input is for the set point, which determines the desired power level. The second input is for the measured value, which, in this case, is the electric power. Instead of using real values, a normalized error approach using a “feedback” component was employed.

This approach works as follows: the measured value signal is sent to the “feedback” component. Simultaneously, a “ramp” signal sends the real power demand level to the “feedback” component, indicating a power decrease. Based on these two power levels, the normalized error is calculated:

$$\varepsilon_{norm} = \frac{P_{measured} - P_{power\ demand}}{P_{power\ demand}} \quad (7.1)$$

The PI controller, which accepts the normalized error, works to minimize the difference between the feedback signal and the set point, aiming to bring this difference to zero. The output signal of the PI controller regulates the valve opening to achieve the minimum error value. The valve opening affects the mass flow rate according to equation 7.2:

$$\dot{m} = K_v \cdot \theta \cdot (p_{in} - p_{out}) \quad (7.2)$$

Where \dot{m} is the mass flow through a valve, K_v – nominal hydraulic conductance, θ – valve opening coefficient.

The PI controller used for the primary side simulates the insertion of control rods to decrease thermal power in the reactor core according to electric power demands. The primary condition for the PI controller is to maintain a fixed average temperature in the primary side. Consequently, the hot leg and cold leg temperatures may vary depending on power generation, but the average temperature must always remain at 295.5°C.

All results are illustrated in Figure 30.

According to utility requirements for light water reactors [23], in extreme cases, the power level must decrease by 3-5% per minute compared to the nominal power. In this experiment, the expected decrease in thermal power is 7%, which is approximately 11 MW. Therefore, the duration of this transient, defined by the “Ramp” source, is set to 3 minutes. The total simulation time is 1200 seconds.

In this model, the electrical power decreases by 5 MW, which is approximately 10%. This results in a power reduction from 55 MW to 50 MW. Such a variation in power leads to changes in the valve opening coefficient from 1 to 0.33. As there is a dependency between the valve opening and the mass flow rate, the flow rate changes from 77.5 kg/s to 71.2 kg/s. Due to the reduction in the cross-sectional area of the valve, the pressure in the secondary side increases inversely proportional to the mass flow rate.

Consequently, according to the energy balance equation, variations in mass flow affect the temperature of the fluid and thermal power. The inlet temperature for feed water remains constant during the simulation, but the outlet temperature begins to increase after 80 seconds of the transient and stabilizes at $T = 311.4^\circ\text{C}$.

Regarding the behavior of cold and hot leg temperatures, it is observed that they tend to maintain the average temperature at a constant level. Therefore, during the power transient, the hot leg temperature decreases while the cold leg temperature increases inversely proportionally. Simultaneously, thermal power decreases by 11 MW.

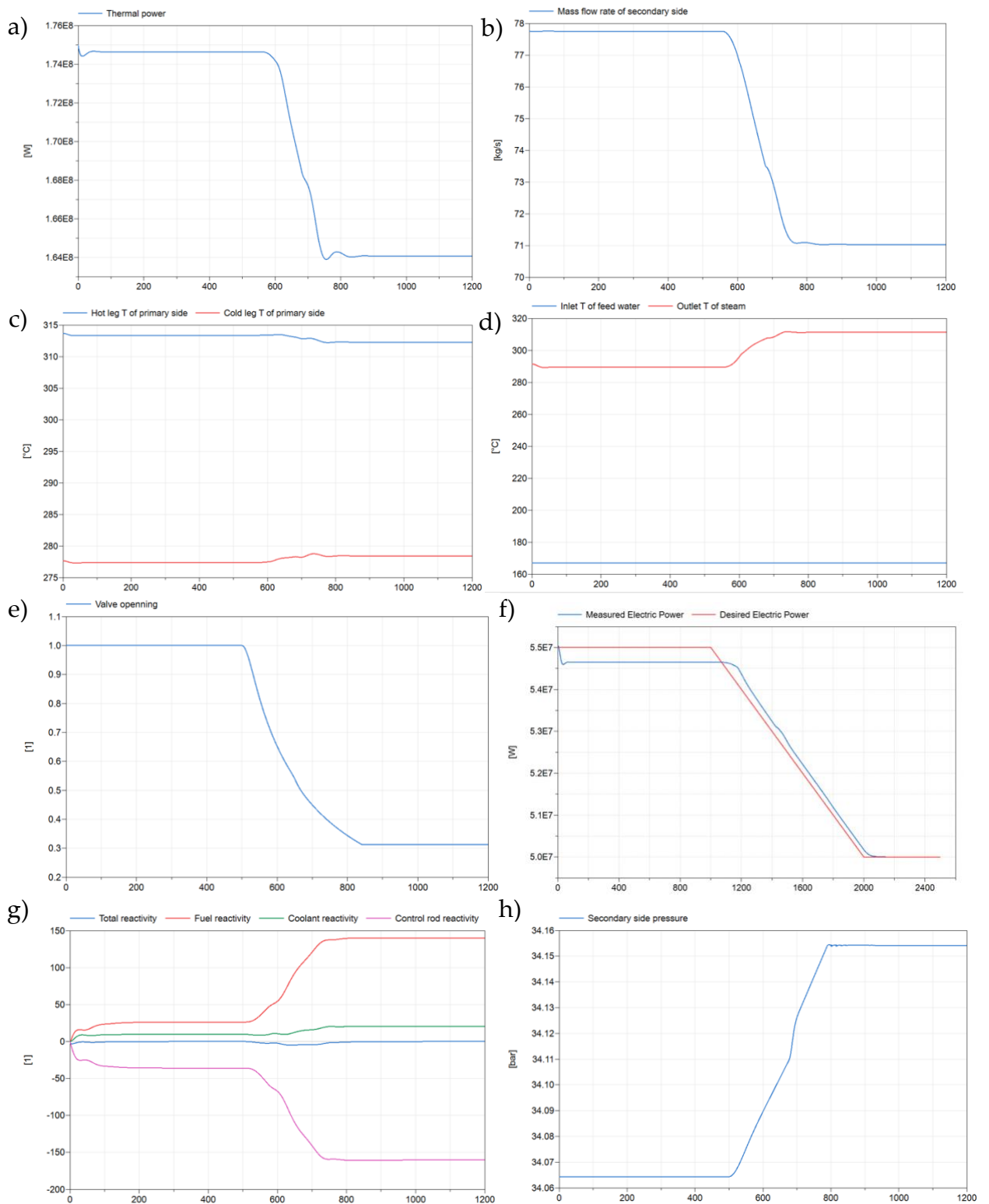


Figure 27: Parameters during load following

a – Thermal power, b – Mass flow rate of secondary side, c – Temperature of coolant, d – Temperature of feedwater/steam, e – Valve opening, f – Power demand vs. measured electric power, g – Reactivity factors, h – Pressure of secondary circuit.

Furthermore, it is illustrated that the reactor remains at critical condition throughout this transient. The total reactivity remains zero because the negative reactivity insertion by control rods, determined by PI control, is compensated by positive reactivity provided

by coolant and fuel due to the decrease in fuel temperature, which mitigates the negative Doppler effect (Equation 6.5).

Some fluctuations of parameters during the transient can be explained by the simulation time. As mentioned above, the duration of the power decrease (180 seconds) is close to the extreme case of utility requirements, which may result in some instabilities during the power reduction. Increasing the duration of the transient (e.g., to 1000 seconds) leads to a smoother transition without any peaks.

7.3 Passive residual heat removal simulation

The third experiment analyzes the passive residual heat removal system (Fig. 31) in a scenario where all control rods are inserted. In this situation, power is generated by fission products rather than by neutron fission. According to the decay power law, at the moment all control rods are inserted, the reactor retains 6% (10.5 MW) of its nominal power, followed by a subsequent exponential decrease:

$$Q_{residual} = 6 \cdot 10^{-2} \cdot Q_{nominal} (\tau^{-0,2} + (\tau + T)^{-0,2}) \quad (7.3)$$

Two assumptions were made:

1. The first temperature source is set to $T = 35^{\circ}\text{C}$, representing the air that removes heat, functioning like the Air Heat Exchanger (AHX).
2. The second temperature source is set to $T = 100^{\circ}\text{C}$, simulating the saturated water in the Emergency Core Cooling (ECC) tank. The liquid entering the steam generator (SG) is subcooled water, but at the outlet, it is converted to saturated steam at $T = 200^{\circ}\text{C}$.

The results of the modeling are illustrated in Figure 31.

Since the Passive Residual Heat Removal System (PRHRS) must operate for several days [8], the system is simulated for a duration of 2 days. In terms of power removal, it can be observed that after $t = 0.003$ days, the Air Heat Exchanger (AHX) removes more power than the water Heat Exchanger (HX). This is reasonable because the AHX interacts with the fluid earlier, and when the power generated by the reactor core is sufficiently low, it can be removed by the AHX alone.

Moreover, due to the use of a constant temperature source, after $t = 0.8$ days, when the temperature of the water drops below 100°C , the water heat exchanger (HX) stops removing power and instead starts to produce power for the safety circuit. It can be assumed that by this time, the stored water in the cistern is exhausted, and the residual heat release can be removed without relying on the water HX. Consequently, the air heat exchanger (AHX) is capable of removing all the energy by itself from that moment onwards.

Such strong design assumptions lead to another consequence: the temperature of the water entering the steam generator (SG) increases because, after $t = 0.8$ days, the PRHRS loop receives energy from the temperature source functioning as the water HX.

However, this does not significantly impact the overall performance quality of the PRHRS, as Figure 31 demonstrates that the results are satisfactory.

Parameters such as steam quality, temperatures, and pressure along the entire circuit path experience a significant drop during the first minutes of the simulation, followed by a smooth decrease until the complete removal of residual power. At the initial moment, the steam quality at the SG outlet is 0.95, at the inlet is 0, and between the AHX and the water HX, the steam quality is 0.55. The initial pressure on the secondary side is 2 MPa.

The mass flow rate shows a smooth increase, which can be explained by the energy balance equation: ΔT decreases faster than thermal power, thus an increase in the mass flow rate compensates for this change.

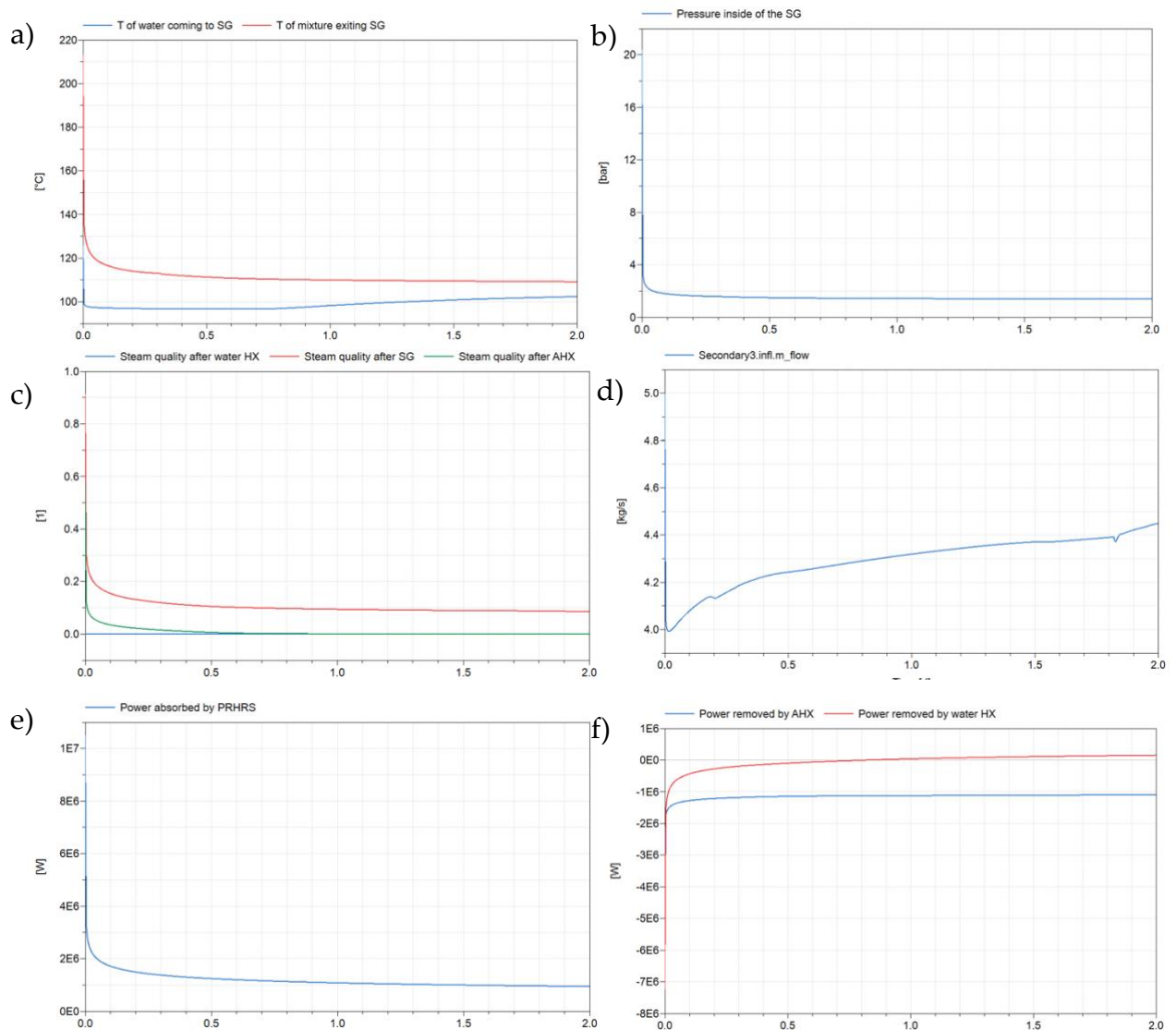


Figure 28: Results of PRHRS simulation

- a – Temperature of secondary side on inlet and outlet, b – Pressure of secondary side, c – Steam quality before and after SG, and between HXs, d – Mass flow rate of secondary side, e – Thermal power received by SG, f – Thermal power removed by AHX and water HX

8 Conclusion and future developments

The SMR RITM-200 model, as described in [4], has been analyzed using the programming language Modelica within the Dymola application. The steady-state simulation of the primary and secondary sides yields accurate results, with values coinciding with reference data. However, a few differences arise due to certain design modifications and simplifications, such as the removal of the "pseudo-regenerative" section in the SG and a 10 cm decrease in the total length of the SG.

Additionally, a load-following simulation was performed, showing the dynamic behavior of the reactor under power reduction up to 10% in an open-loop system. The system demonstrated the feasibility of linking valve operation with a control system based on electric power input.

The pressure drops across all major components of the passive residual heat removal system (PRHRS) were also investigated to analyze the removal of residual heat in the event of complete control rod insertion. The system performed adequately, even under strong assumptions such as using temperature sources instead of models of real heat exchangers.

Looking ahead, the system simulating the load-following process needs further refinement. The circuit should be closed, incorporating all components such as heat exchangers, deaerators, and pumps with their complete geometrical features, which are currently not available in open sources.

The PRHRS must be coupled with the primary circuit of the RITM-200 to demonstrate the direct removal of thermal power from the reactor core. Furthermore, the simplified heat exchangers should be replaced with real heat exchangers using accurate fluid properties. To achieve this, the code needs to be enhanced using a more advanced modeling application.

Bibliography

- [1] M. K. Rowinski, T. J. White, and J. Zhao, "Small and Medium sized Reactors (SMR): A review of technology," *Renewable and Sustainable Energy Reviews*, vol. 44. Elsevier Ltd, pp. 643–656, 2015. doi: 10.1016/j.rser.2015.01.006.
- [2] Nuclear energy agency, "Small Modular Reactors: Challenges and Opportunities," 2021.
- [3] G. Locatelli, C. Bingham, and M. Mancini, "Small modular reactors: A comprehensive overview of their economics and strategic aspects," *Progress in Nuclear Energy*, vol. 73, pp. 75–85, May 2014, doi: 10.1016/j.pnucene.2014.01.010.
- [4] ROSATOM, "ROSATOM SMR SOLUTIONS RITM SERIES," 2019.
- [5] D. L. Zverev *et al.*, "Reactor Installations for Nuclear Icebreakers: Origination Experience and Current Status," *Atomic Energy*, vol. 129, no. 1, pp. 18–26, Nov. 2020, doi: 10.1007/s10512-021-00706-x.
- [6] V. M. Belyaev, A. N. Pakhomov, and K. B. Veshnyakov, "Status of SMR development and deployment of SMRs in the Russian Federation," 2019.
- [7] V. V. Petrunin, Y. P. Fadeev, A. N. Pakhomov, K. B. Veshnyakov, V. I. Polunichev, and I. E. Shamanin, "Conceptual Design of Small NPP with RITM-200 Reactor," *Atomic Energy*, vol. 125, no. 6, pp. 365–369, Apr. 2019, doi: 10.1007/s10512-019-00495-4.
- [8] W. Surip, N. Putra, and A. R. Antariksawan, "Design of passive residual heat removal systems and application of two-phase thermosyphons: A review," *Progress in Nuclear Energy*, vol. 154. Elsevier Ltd, Dec. 01, 2022. doi: 10.1016/j.pnucene.2022.104473.
- [9] D. Zverev, A. Pakhomov, and V. Polynichev, "A NEW GENERATION RITM-200 REACTOR PLANT FOR A PROMISING NUCLEAR ICEBREAKER," 2012.
- [10] Atomenergomash, "SOLUTIONS FOR THE SHIPBUILDING INDUSTRY," 2010.
- [11] S. Boarin *et al.*, "Object-Oriented Modeling and simulation of a TRIGA reactor plant with Dymola," in *Energy Procedia*, Elsevier Ltd, Nov. 2016, pp. 42–49. doi: 10.1016/j.egypro.2016.11.006.
- [12] D. E. Savitsky and A. V. Kuzmin, "The calculation of the campaign of reactor RITM-200," in *IOP Conference Series: Materials Science and Engineering*, IOP Publishing Ltd, Jan. 2021. doi: 10.1088/1757-899X/1019/1/012057.
- [13] V. I. Korolev, "ANALYSIS OF NEW TECHNICAL SOLUTIONS FOR THE RITM-200 REACTOR PLANT IN THE PROJECT 22220 OF UNIVERSAL NUCLEAR ICEBREAKERS," *Vestnik Gosudarstvennogo universiteta morskogo i rechnogo flota imeni admirala S. O. Makarova*, vol. 14, no. 6, pp. 945–960, Dec. 2022, doi: 10.21821/2309-5180-2022-14-6-945-960.

- [14] A. Zakharychev, G. Iksanova, and A. Kupriyanov, "METHODODOLOGICAL ISSUES AND SOME EXPERIMENTAL RESULTS AND COMPUTATIONAL STUDIES OF CRITICAL HEAT FLOWS IN THE FUEL ASSEMBLY OF THE RITM-200 REACTOR," 2021.
- [15] N. V. Nikitin, "Marine intellectual technologies," 2020.
- [16] H. Zhang, Y. Li, Y. Zhao, J. Wang, S. Du, and W. Ma, "Modeling and simulation of a micro gas-cooled nuclear reactor using Modelica," *Front Energy Res*, vol. 11, 2023, doi: 10.3389/fenrg.2023.1206755.
- [17] H. L. J. Duderstadt James J., "Nuclear reactor analysis," 1976.
- [18] Idelchik I. E., "Handbook of hydraulic resistance," 1992.
- [19] M. M. Shah, "Improved General Correlation for Condensation in Channels," *Inventions*, vol. 7, no. 4, Dec. 2022, doi: 10.3390/inventions7040114.
- [20] W. Song, Z. Peng, P. Li, P. Shi, and S. B. Choi, "Annular surface micromachining of titanium tubes using a magnetorheological polishing technique," *Micromachines (Basel)*, vol. 11, no. 3, Mar. 2020, doi: 10.3390/mi11030314.
- [21] A. Lokhov, "Technical and Economic Aspects of Load Following with Nuclear Power Plants," 2011. [Online]. Available: www.oecd-nea.org
- [22] J.-C. Shen, "New tuning method for PID controller," 2002.
- [23] S. Popov, J. Carbajo, V. Ivanov, G. Yoder, "Thermophysical properties of UO₂ fuel", *National technical information service*, 1996.
- [24] Mitsubishi Heavy Industries, Ltd., "Mitsubishi fuel design criteria and methodology", US-APWR Topical Report, May 2007.

List of Figures

| | |
|---|----|
| Figure 1: Classification of SMR..... | 2 |
| Figure 2: SMR key economic drivers to compensate for diseconomies of scale..... | 3 |
| Figure 3: Advantages of SMR | 4 |
| Figure 4: Life cycle of offshore NPP..... | 6 |
| Figure 5: Steam-generation block of the RITM-200 reactor installation. | 9 |
| Figure 6: Layout of land-based RITM-200 | 10 |
| Figure 7: RHRS and SIS arrangement..... | 13 |
| Figure 8: Schematic diagram of the passive residual heat removal system in RITM-20014 | |
| Figure 9: SGU general view..... | 16 |
| Figure 10: Fuel assembly of RITM-200: | 19 |
| Figure 11: General view of the fuel assembly:..... | 19 |
| Figure 12: Scheme of the steam generating cassette of the steam generator RU "RITM-200" | 20 |
| Figure 13: Scheme of feed water supply and steam removal from the module | 21 |
| Figure 14: Scheme of primary and secondary scheme of RITM-200..... | 12 |
| Figure 15: Model of RITM-200 | 49 |
| Figure 16: Model of reactor system. | 50 |
| Figure 17: Radial heat transfer modelling..... | 52 |
| Figure 18: Model of steam generator | 20 |
| Figure 19: Temperature distribution of primary and secondary fluids without pseudo-regenerative region..... | 57 |
| Figure 20: Model of secondary circuit made in EBSILON professional | 58 |
| Figure 21: Model of steam turbine with separator..... | 58 |
| Figure 22: Model of feed water part of secondary circuit..... | 60 |
| Figure 23: Model of deaerator..... | 61 |
| Figure 24: Radioactive decay law | 62 |
| Figure 25: Passive residual heat removal model..... | 63 |
| Figure 26: ECD tank | 28 |
| Figure 27: Model of PRHRS with temperature boundary conditions..... | 32 |
| Figure 28: Results of steady state simulation of primary and secondary sides..... | 69 |

| | |
|---|----|
| Figure 29: Model of load following simulation | 71 |
| Figure 30: Parameters during load following..... | 51 |
| Figure 31: Results of PRHRS simulation | 75 |

List of Tables

| | |
|---|----|
| Table 1: Characteristics of OK-150 | 7 |
| Table 2: Main technical characteristics of OK-900 | 7 |
| Table 3: Characteristics of KLT-40M..... | 8 |
| Table 4: Characteristics of RITM-200 | 9 |
| Table 5: Main technical characteristics of RITM-400 | 10 |
| Table 6: Characteristics of RITM-200 | 11 |
| Table 7: General characteristics of SG unit..... | 15 |
| Table 8: Amount of SGU's components | 17 |
| Table 9: Parameters of reactor core | 18 |
| Table 10: Main design characteristics of steam generator | 22 |
| Table 11: The main technical characteristics of the K-50-3,4/50 turbine | 23 |
| Table 12: Stodola's coefficient and pressures of each stage of turbine. | 59 |
| Table 13: Gravitational and frictional pressure drop of PRHRS..... | 66 |
| Table 14: Local pressure drops of PRHRS..... | 68 |
| Table 15: Comparison of reference and modelled data..... | 69 |

List of symbols

| Variable | Description | SI unit |
|------------------|--|-------------------------------|
| c_p | Specific heat capacity | $\frac{J}{kg \cdot ^\circ C}$ |
| T | Temperature | $^\circ C$ |
| k | Conductivity | $\frac{W}{m \cdot K}$ |
| N | Neutron density | $\frac{neutrons}{cm^3}$ |
| t | Time | s |
| ρ | Reactivity | dimensionless |
| β | Delayed neutron fraction | dimensionless |
| Λ | Neutron generation time | s |
| λ | Decay constant of the delayed neutron precursors | $\frac{1}{s}$ |
| C_i | Concentration of delayed neutron precursors | $\frac{neutrons}{cm^3}$ |
| ρ_{init} | Initial reactivity | dimensionless |
| ρ_{fuel} | Fuel reactivity | dimensionless |
| ρ_{Xe} | Xenon reactivity | dimensionless |
| ρ_{CR} | Control rod reactivity | dimensionless |
| $\rho_{coolant}$ | Reactivity of coolant | dimensionless |
| α_f | fuel feedback coefficient | dimensionless |
| α_c | Coolant feedback coefficient | dimensionless |
| N_I | Concentration of I-131 | $\frac{atoms}{cm^3}$ |

| | | |
|-----------------|--|--|
| γ_I | Yield of Iodine | $\frac{\text{atoms}}{\text{fission}}$ |
| Σ_f | Fission macroscopic cross-section | $\frac{1}{\text{cm}}$ |
| ϕ | Neutron flux | $\frac{\text{neutrons}}{\text{cm}^2 \cdot \text{s}}$ |
| λ_I | Decay constants of Iodine | $\frac{1}{\text{s}}$ |
| N_{Xe} | Concentration of Xe-135 | $\frac{\text{atoms}}{\text{cm}^3}$ |
| γ_{Xe} | Yield of Xenon | $\frac{\text{atoms}}{\text{fission}}$ |
| λ_{Xe} | Decay constants of Xenon | $\frac{1}{\text{s}}$ |
| σ_a^{Xe} | Microscopic capture cross-section | cm^2 |
| ν | Number of emitted neutrons per fission | $\frac{\text{neutrons}}{\text{eV}}$ |
| c_t | Reactivity adjustment factor | eV |
| ρ | Density of material | $\frac{\text{kg}}{\text{m}^3}$ |
| r | Radius | m |
| q''' | Specific power | $\frac{\text{W}}{\text{m}^3}$ |
| h_{gap} | Heat transfer coefficient of the gap | $\frac{\text{W}}{\text{m}^2 \cdot \text{K}}$ |
| Q | Power | W |
| δ_{gap} | Thickness of the gap | m |
| k_{gap} | Filling gas conductivity | $\frac{\text{W}}{\text{m} \cdot \text{K}}$ |
| A | Cross section area of the coolant flow | m^2 |
| Pitch | Pitch of tubes in the assembly | m |

| | | |
|------------------------|--|--------------------------|
| w_{in} | Inlet mass flow rate | $\frac{kg}{s}$ |
| M | Mass of a medium | kg |
| w_{out} | Outlet mass flow rate | $\frac{kg}{s}$ |
| N_t | Number tubes | amount |
| L | Length of tube | m |
| p_{out} | Outlet pressure | Pa |
| p_{in} | Inlet pressure | Pa |
| $\Delta p_{st.head}$ | Static head pressure drop | Pa |
| $\Delta p_{friction}$ | Frictional pressure drop | Pa |
| $h[i]$ | Enthalpy in each volume | $\frac{J}{kg}$ |
| $Q_{single}[i]$ | Heat flows entering the volumes for a single tube. | W |
| f | Fanning friction factor | dimensionless |
| G | Mass flux | $\frac{kg}{s \cdot m^2}$ |
| \emptyset | Diameter of tube | m |
| g | Acceleration due to gravity | $\frac{m}{s^2}$ |
| Nu | Nusselt number | dimensionless |
| Re | Reynolds number | dimensionless |
| Pr | Prandtl number | dimensionless |
| q' | Linear heat rate | $\frac{W}{m}$ |
| Wall resistance | Thermal resistance of a wall | $\frac{K}{W}$ |
| K_t | Stodola's coefficient | dimensionless |
| η_{iso} | Isentropic efficiency | dimensionless |

| | | |
|----------------|---|-------------------------|
| η_{mech} | Mechanical efficiency | dimensionless |
| P_m | Mechanical power | MW |
| ω | Shaft angular velocity | $\frac{rad}{s}$ |
| τ | Net torque acting on the turbine | dimensionless |
| h_{iso} | Isentropic outlet enthalpy | $\frac{J}{kg}$ |
| E | Internal energy | J |
| K | Global heat transfer coefficient | $\frac{W}{K}$ |
| ΔT | Logarithmic mean temperature difference | dimensionless |
| $Q_{residual}$ | Residual power | W |
| $Q_{nominal}$ | Nominal power | W |
| T | Operational time | s |
| h_{TP} | Two-phase heat transfer coefficient | $\frac{W}{m^2 \cdot K}$ |
| ρ_L | Density of liquid | $\frac{kg}{s}$ |
| ρ_G | Density of gas | $\frac{kg}{s}$ |
| μ_L | dynamic viscosity of liquid | $\frac{Pa}{s}$ |
| Z | Shah's correlating parameter | dimensionless |
| P | Pressure | Pa |
| $P_{reduced}$ | Reduced pressure | Pa |
| x | Steam quality | dimensionless |
| D_{hydr} | Hydraulic diameter | m |
| $\bar{\Delta}$ | Roughness of surface of tube | m |
| ζ_M | Coefficient of local resistance | dimensionless |

| | | |
|----------------------|-------------------------------|-------------------|
| $A_1 B_1 C_1$ | Local coefficients | dimensionless |
| ε_{norm} | Normalized error | dimensionless |
| $P_{measured}$ | Measured electrical power | W |
| $P_{power\ demand}$ | Power demand | W |
| K_v | Nominal hydraulic conductance | $\frac{kg/s}{Pa}$ |
| θ | Valve opening coefficient | dimensionless |

Acknowledgments

Firstly, I would like to thank Professor Marco Enrico Ricotti and Professor Stefano Lorenzi for giving me this excellent opportunity to work on the topic of the SMR.

Thanks to Guido Carlo Maratti for the assistance related to modeling in Modelica language with the Dymola simulation environment.

Secondly, I would like to thank all my professors at the university for imparting their knowledge to me as part of the master's program of Nuclear Engineering.

Conclusively, I would like to thank my family for their consistent support throughout my journey.